
Identification of myocardial infarction by high-frequency serial ECG measurement

Master's thesis

University of Turku

Department of Computing

Master's in Health Technology

2022

Jonas Sandelin

Supervisors:

Tero Koivisto

Matti Kaisti

UNIVERSITY OF TURKU
Department of Computing

Jonas Sandelin: Identification of myocardial infarction by high-frequency serial ECG measurement

Master of Science Thesis, 74 p.
Medical Analytics and Health IoT
February 2022

The purpose of this study is to attempt to identify acute myocardial infarction with high frequency serial electrocardiogram. High-frequency ECG and serial ECG are both unique ECG analysing techniques. The idea in this study is to combine these two and see if changes between different ECGs from the same person can provide us some information, whether it being in the high-frequency or normal frequency range of the ECG.

To answer the questions, an existing database which contained multiple ECGs for each person with high sampling frequency was used. 5 different machine learning models were trained and tested with this database. The results of the machine learning methods were good, producing the mean accuracy of 91.9%, while the best model was the Extra Trees machine learning model. It produced the accuracy of 97.9% when applying cross-validation to the database.

After these results, high-frequency serial ECG could be stated to be relevant. However, having ECG measured regularly can be expensive and time consuming. Therefore, the possibility of using a wearable ECG device was also studied. With a device called SAFE, developed by the University of Turku, a new high-frequency serial ECG database was gathered. The already existing machine learning model trained with the previous data was applied to this database and produced a mean accuracy of 90%. The quality of the ECGs gathered with the device were also deemed to be viable. Both high-frequency ECG and serial ECG were found to be relevant methods. A wearable device could be used for AMI detection if the ECG is sufficient enough. Future studies could include increasing the dataset size of the wearable device, investigate other myocardial diseases and exploring the possibilities of high-frequency ECG further.

Keywords: electrocardiography, acute myocardial infarction, machine learning, wearables, classification, health monitoring, serial ECG, high-frequency ECG

Table of Contents

1 Introduction	1
1.1 Research questions	3
2 Literature	4
2.1 Electrocardiography	4
2.1.1 Serial electrocardiography	7
2.1.2 High-frequency electrocardiography	9
2.2 Acute myocardial infarction	12
2.3 Available methods	14
2.3.1 AliveCor	15
2.3.2 HeartBeam	16
2.3.3 RELF Project	17
2.3.4 AngelMed	18
2.3.5 Smartwatches	19
2.4 Machine learning methods	20
2.4.1 K-Nearest neighbors	21
2.4.2 Support Vector Machine	22
2.4.3 Decision Tree	23
2.4.4 Random Forest	24
2.4.5 Extra Trees	24
2.5 Cross-validation	25
3 STAFF III	26
3.1 Database	26
3.2 Comparing different ECGs	29
4 Signal processing	31
4.1 Pre-processing the data	31
4.1.1 Filtering	32
4.1.2 Normalization	33
4.2 Peak detection	34
4.2.1 R-peak detection	34
4.2.2 P-, Q-, S- and T-wave detection	37
4.3 Average waveform	41
4.3.1 HF Average waveform	42
4.4 P-average waveform	42
4.4.1 HF P-average waveform	43
4.5 Segmentation	44

5 Feature extraction and selection	47
5.1 Feature extraction	47
5.2 Feature selection	49
6 SAFE	51
6.1 SAFE device	51
6.2 Taking measurements/Data gathering	53
7 Results	55
7.1 Results of STAFF database	55
7.2 Results of SAFE vs STAFF	57
7.3 Data analysis	59
7.3.1 Principal component analysis	60
7.3.2 Box plots.....	61
8 Conclusions	64
References	66
Attachments	73
STAFF III database annotations	73

1 Introduction

Acute myocardial infarction is one of the biggest health problems all over the world [1][2][3][4]. More commonly known as heart attack, acute myocardial infarction can lead to sudden death or cause disabilities and structural damage to the heart muscle [1]. It can be detected with different techniques, but one of the basic detection methods for myocardial infarction is electrocardiogram (ECG) [5][6]. Over the years while the technologies have advanced, ECG has also increased its importance [5]. The most used type of ECG is the standard 12-lead ECG [7][8]. It includes 12 leads, 6 precordial leads, 3 limb leads and 3 augmented leads from these limb leads [5]. While ECG is usually the key when detecting myocardial infarctions, it can be deceptive and has multiple flaws. The diagnostic accuracy from the ECG is low and the variability of interpretation is high [2]. The variability between patients can also be high [9] and can cause false predictions. Also, some changes cannot be found in the ECG, because the time period during the ECG recording is not usually long enough.

One solution to overcome these problems is serial electrocardiogram (S-ECG). In short, in S-ECG we compare different ECG recordings from one individual with each other [7][9][10][11]. It has been noticed to perform better than the initial ECG, when detecting myocardial infarctions [2][12]. What makes S-ECG great is that, when comparing the ECGs of the same patient, we remove the possibility of variability between patients. The time interval between the different recordings can vary from 5 minutes to even years [2][13][11]. This means that we get a more in-depth look into the clinical myocardial health of the patient [7] and the possible changes of the ECG are shown clearer than in the initial recording. These changes can be analysed visually or with different algorithms such as machine learning for example. However, the S-ECG based automatic algorithms are yet to be as practical as the single ECG algorithms [7]. Multiple different S-ECG features can reveal a possibility of a cardiac disease [10], especially with machine learning algorithms. Especially ST-segment changes have been used to detect acute myocardial infarctions [1][6]. With a single ECG recording, the changes in the ST-segment might not be found easily, but with S-ECG these changes can be detected easier [1].

Another method used in this thesis is high-frequency ECG (HF-ECG). It has been noticed to provide more in-depth look into the myocardial health of the patients [8][14]. This method focuses on the higher frequency ranges of the ECG, above 150 Hz [8][15][16]. The idea in this thesis is to combine

the HF-ECG methods with the S-ECG. This type of combination is almost unique, and similar studies could not be found. Only a few studies bearing similarities to ours could be found and they did provide evidence that a high-frequency serial ECG could be a viable option detecting myocardial infarction [17][18][19].

Some studies suggest that a yearly ECG with serial measurement could be useful to detect heart failure and myocardial infarctions [13]. However, we believe that even a weekly measurement would be highly beneficial, but the trouble going to the hospital to get your ECG measured is not worth it. That is why in this study we use a small and wearable device called “SAFE” to measure ECG. The possibility of measuring ECG at home regularly or when feeling chest pain, could save multiple lives. These kinds of wearable ECG devices could also monitor ECG continuously and alarm the patient when the signal shows signs of disease [20]. Technologies have only been advancing over the past centuries [5] and it’s only a matter of time when continuously measuring wearable ECG will become a trend. Interest in self-monitoring health has been increasing in the recent years, and these kinds of solutions have already been used to detect atrial fibrillation successfully [21]. These results are sort of irrelevant for myocardial infarctions but prove that heart’s irregularities can be detected with wearable device.

In this thesis, we will develop a method to detect acute myocardial infarctions with serial electrocardiography. We try to classify between a healthy subject and a subject suffering from myocardial infarction with 5 different machine learning methods. To create the features to input for the machine learning methods, we will extract features from two ECG recordings from the same patient. After this, the features for S-ECG will be calculated. For the data we will be using an existing database as well as creating our own with the wearable SAFE device.

The thesis is structured as follows: first chapter will introduce the problem in hand and explain the reasoning behind this thesis. Second chapter will go through the literature including general information and theories, and also the work done before. Chapter 3 presents the database used in this study. Chapter 4 goes through our signal processing and what do we extract from the signal. Chapter 5 goes through the feature extraction and selection process. Chapter 6 introduces the SAFE device and data that was gathered with it. Chapter 7 goes through the results. Chapter 8 explains the results briefly and concludes the thesis.

1.1 Research questions

In this thesis we have two research questions. Research question 1: Can serial electrocardiogram detect acute myocardial infarction? This will be answered by creating machine learning models based on an existing database. Research question 2: Can a wearable ECG device be used for detecting acute myocardial infarction with serial electrocardiogram? This will be answered by using the created machine learning model to classify the data gathered with our own wearable ECG device. Answers for these questions can be found in chapter 8.

2 Literature

2.1 Electrocardiography

The 12-lead electrocardiogram measurement is one the most essential parts of medical care [5][7][8][22]. Different heart diseases, like acute myocardial infarction, are a significant cause of death all over the world [1][2][4]. These diseases can possibly be diagnosed with ECG and then treated accordingly. ECG is a vital part when detecting acute myocardial infarction [6]. ECG, or also abbreviated to EKG [22], measures the electrical activity of the heart. Furthermore, ECG signal is the myocardial electrical activity on the body surface [23]. For every individual, ECG is a fairly periodic signal [23]. The basic 12-lead ECG consists of six precordial leads V1-V6, three limb leads I-III and three augmented limb leads aVR, aVL and aVF [5]. Normally, ECG is measured with bandwidth of 0.05 to 150 Hz with adults [5]. This can be extended to 250 Hz with children. ECG consists of many easily distinguishable characteristics, such as the P-wave, QRS-complex and T-wave [5][22][23]. It is important to detect these peaks since their timings and other features might be an indicator of bad health [23]. Figure 1 represents a typical ECG recording.

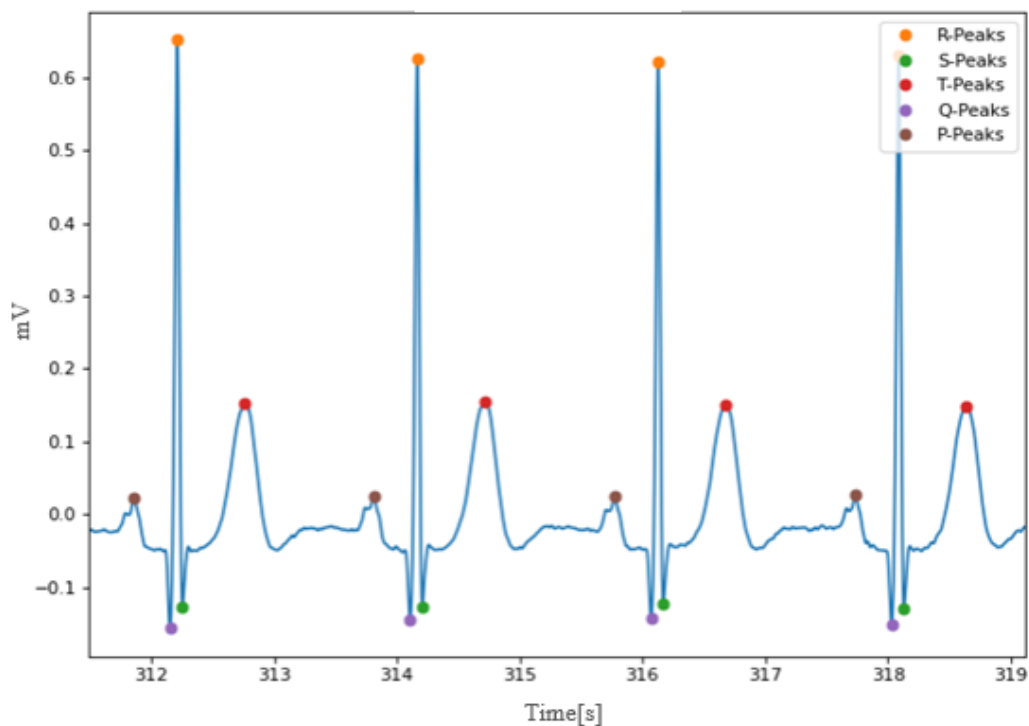


Figure 1. ECG from STAFF III database. Signal represents patient 71 ECG from lead II.

The most distinguishable and important part of the ECG is the QRS-complex and especially the R-peak. The QRS-complex represents the depolarization of the ventricles [5][22]. This refers to the moment where the heart pumps blood from the myocardium to the rest of the body and lungs. R-peak also contains the repolarization of the atria, but it can't be further detected due to the much higher amplitude of the depolarization of the ventricles [5]. QRS-complex consists of three parts, Q-peak, R-peak, and S-peak. The Q-peak is the dipping point before the initial R-peak. In figure 1 we can see it very clearly, but sometimes it is harder to spot. The R-peak is the highest point of the QRS-complex. Detecting the QRS-complex and the R-peaks especially is a vital part of processing and analysing the ECG [24]. Every QRS-complex represents ventricular beat and with the rate of those beats, we can calculate the heart rate of the patient. Real-time R-peak detection is important for patients with heart diseases [24], so that the changes happening in the signals can be seen as soon as possible. One point to notice is that the R-peak is always positive [23], while the other peaks can be negative. After the QRS-complex has reached its R-peak, it starts to come back down again. It then produces another dip, similar to the Q-peak. This lowest point is called the S-peak or the S-wave.

Before the QRS-complex we can see a small peak in the ECG. This is called the P-peak or the P-wave. P-wave represents the moment of atrial depolarization [5][22]. By myocardial definition, it means the moment where the blood is pumped from the atria to the ventricles. Changes in the P-wave can tell different things. Since the P-wave represents the myocardial electrical activity of the atria, it can be studied to detect diseases concerning the myocardial atria. One example of this kind of disease is atrial fibrillation, which is commonly detected from the P-wave [25]. In atrial fibrillation, the P-wave is usually absent. The duration, height and variability of the P-waves can be predictors of atrial fibrillation [25]. The PR-segment, segment between P-wave and R-peak, can also reveal some abnormalities in the atrial myocardia [22].

After the QRS-complex there is another peak called the T-peak or the T-wave. This represents the repolarization of the ventricles [5][22]. This happens because after the depolarization of the ventricles, the ventricles relax, which produces a signal strong enough to be seen in the ECG [22]. As it was with P-wave, changes in the T-wave can be a sign of myocardial disease. One of the most common myocardial diseases which takes advantage of T-wave detection is acute myocardial ischemia. When prolonged, myocardial ischemia can lead to myocardial infarction, which is one of the biggest reasons of death in the world [1][2][4]. By monitoring the changes in the ST-segment, which is the segment between the S-peak and the T-wave, we can detect ischemia. It is one of the basic approaches to detect ischemia [6][15][14]. The altitude, length and variability of the segment can be signs of ischemia. ST-elevation is shown in figure 2.

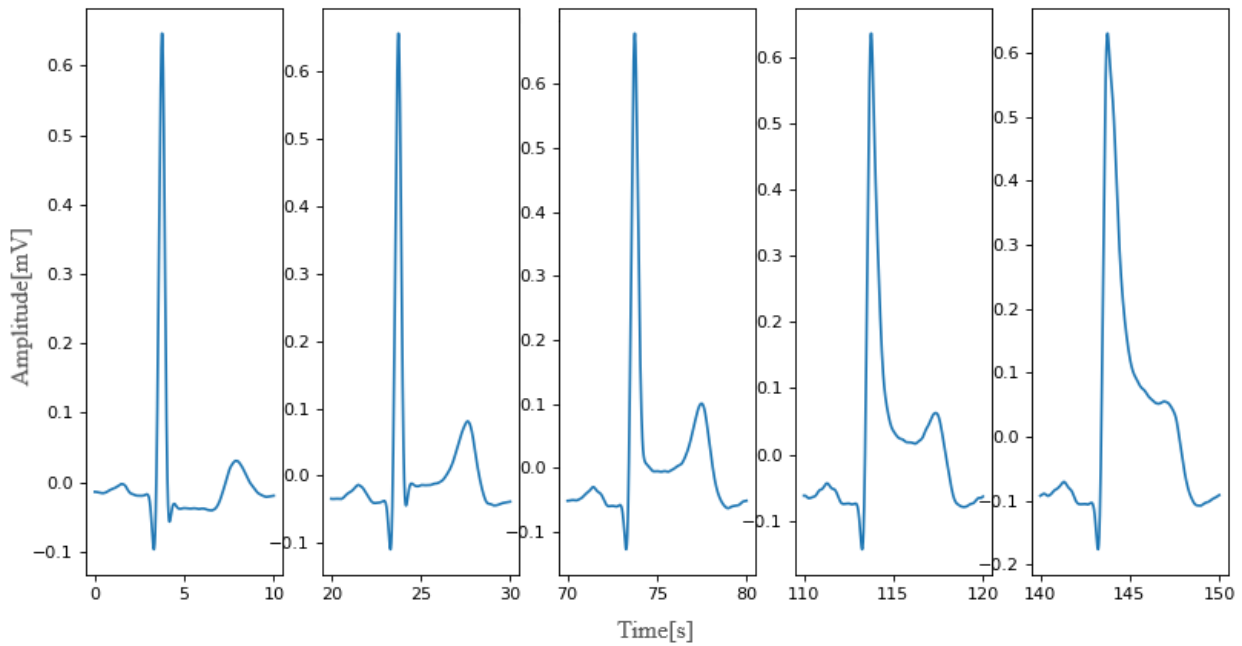


Figure 2. ST-elevation. From STAFF III database, recording 44c lead V5. Every figure represents average waveform of the certain timeperiod.

All these events are initiated by the sinoatrial node (SA node), also called the pacemaker of the heart [22][26]. These regular events can be predicted because the SA node creates electrophysiological events in the myocardia, which can be seen in the ECG [22]. Heart's job is to pump blood regularly to the rest of the body and SA node helps with that by sending action potentials to the atria, causing the depolarization of the atria, P-wave, to happen [22]. It then fires electric signals to the atrioventricular node (AV node), which then causes the depolarization of the ventricles. This produces the electrical activity of the heart which can then be measured with the device called electrocardiograph [22]. A simple definition of how ECG device works is that it measures the electric difference between two points in the body. These differences are measured with electrodes placed on the skin of the patient [27]. A typical ECG device has an amplifier, which amplifies the low-amplitude signals from the electrodes [27]. After the amplification the signal goes through low-pass-, high-pass- and notch-filters to reduce the possible noise [27]. Low-pass- and high-pass-filters usually filter between 0.5 – 150 Hz, while the notch-filter tries to get rid of any possible powerline noise within the range of 50-60 Hz. After the filtering, the signal is then converted from analog to digital [27]. After this the signal can be displayed and analysed. Because of this, ECG can be defined as a series of electrophysiological events and technological processes to unravel those events [5]. Usually after the acquisition of ECG, it is processed further. Filtering out noise from different sources is important. Due to noise caused by muscle contraction and other artefacts ECG can be further filtered to 0.5 to 40 Hz range [28][29]. The low cut-off frequency of 0.5 Hz can be explained by physiology of the

heart. Normal heart rate is over 40 beats per minute (bpm), which means that the heart is beating at least once every 1.5 seconds [29]. This is 0.67 Hz, which makes it impossible to have any ECG features existing under 0.67 Hz [29]. The high cut-off frequency is explained by cutting off the noise generated by the muscles and electrical noise of 50-60 Hz.

The importance of ECG has been rising for the past few centuries [5]. Detection of acute myocardial ischemia is more reliable than ever and ECG is a vital part of that [5]. However, even though the technology to measure ECG [5] and the algorithms to analyse it have advanced in the recent years, the interpretative variability is high and the diagnostic accuracy is relatively low [2]. Also the intervariability between the patients' ECG signals has to be taken into account when diagnosing the ECG [9].

2.1.1 Serial electrocardiography

As established, the standard 12-lead ECG is an important tool in diagnosing patients with myocardial diseases, but the diagnostic accuracy is not the highest [2]. A solution for this could be serial electrocardiography. Serial electrocardiography (serial ECG, S-ECG) refers to the method of comparing two different ECGs from the same patient to each other [9][10][7]. This method has the potential to e.g. increase the detection rate of acute myocardial infarction for example [2]. Initial ECG can vary a lot between patients in normal population and that can cause some difficulties in interpreting ECGs correctly [9]. Especially machine learning methods can have difficulties interpreting these ECG signals from different patients. This means that variability between patients should be disposed of and focus more on the intraindividual variability [9]. This misinterpretation can be bypassed by comparing different ECGs from the same patient between each other. The first ECG creates sort of an anchor, to which the second ECG will then be compared. The comparison between these two or more ECGs from the same individual is called serial electrocardiography [7][10]. This method has shown promising results and features extracted from the serial ECG have been noticed to reveal changes in the clinical cardiac status of the patient [10]. When comparing standard 12-lead S-ECG to the initial 12-lead ECG where the predictions and the detection of myocardial diseases are made with only one ECG recording from the patient, S-ECG was noticed to be performing better at detecting acute myocardial infarction [12]. Aim of the serial ECG is to show the possible changes in the ECG signals [7]. These changes can be a sign of myocardial disease or pathologies, especially if the change is noticeable. When detecting these changes, usually a visual assessment by the doctors is done for the two ECGs to find possible differences [7]. However, there are some algorithms that calculate the differences and make the analysis based on the calculated

differences [2][7]. Even some commercial solutions support serial ECG analysis by comparing the initial ECG recording to one done previously [7]. In this study, the comparison will be done both visually and with algorithms calculating the differences in the features of ECGs.

One way to compare the serial ECGs is to monitor the changes of the main features of ECG between the different ECGs. One of these features is the ST-segment. As stated before, ST-segment changes are an approved way to detect myocardial ischemia [6][15][14]. The ST-segments elevation, length and deviation can all be monitored between the different ECG recordings. It is easier to detect these ST-segment changes when comparing to a previous recording, since the differences might be clearer than with initial ECG. It is helpful to have a previous ECG recording when detecting acute myocardial infarctions [1]. The volume of ST-segment change can be extracted from S-ECG and then analysed [11]. In some algorithms, if the computer calculates the change to be drastic enough, then it will alarm the person measuring the ECG and will then be further analysed by a doctor [11]. The ST-segmentation is based on the S-wave and T-wave detection algorithms, so there might be some miscalculations. This is why some suggest that all 12-leads should be used to get the best possible result and to eliminate the possible distorted segments from some leads [11]. Comparing the features of S-ECGs is beneficial since the ECGs are taken at different times. The patient is the same and the equipment should be the same which means that in a perfect world the only variability factor is the electrical activity of the heart of the patient.

S-ECG can be done with the same exact equipment as the normal ECG, with electrocardiographic machine [11], so this method can improve the accuracy at a very low cost [2]. One thing to note is that there can be some variability between ECG devices, so the different ECG recordings have to be recorded with the same or at least similar equipment. The previous ECGs, or just one baseline ECG from the patient, need to be saved into a specific patients database where they can later be used as a comparison for the new ECG and to produce the S-ECG. This helps organizing the data and makes the comparison process much easier.

The rate of measuring the ECGs varies a lot. It is up to the clinician to determine the rate of the measurements [11]. If the situation needs it, then the individual ECGs can be recorded within minutes apart from each other [2][11], but if time is not a concern, the ECGs can be measured with a longer period between the recordings [11]. One study has found that even really long interval times can give decent results [13]. This study had the mean interval time of 3.8 years between the recordings. However, they suggested that a yearly ECG recording would be a more reliable solution [13]. There does not seem to be an optimal rate at which to acquire the different ECG recordings [6]. However,

most S-ECG solutions have been found to be working in spite of which rate of measurements has been taken. From a few minutes to a few years, S-ECG seem to be improving the performance of detecting myocardial diseases compared to the initial ECG [2][12][11]. In some cases, if the diagnosis from the initial ECG is ambiguous, S-ECG could be a useful tool [6]. Even though the S-ECG seems to be a promising way to improve diagnosis of myocardial diseases [10], it's real value is yet to be determined [12]. There have not been enough studies yet to determine if S-ECG is a relevant way to detect and monitor myocardial diseases, but it shows great promise and is proven to be a viable option in some studies [2].

2.1.2 High-frequency electrocardiography

The standard 12-lead ECG usually has a bandwidth of 0.5 Hz to 150 Hz [5]. This is usually even further filtered to 0.5-25 Hz for example, when processing the signal. This does get all the required information from the ECG recording, but higher frequencies can give information too. The changes of the health of the heart usually can be found in the electrical activity of the heart, but sometimes they can't be seen in the normal frequency range of ECG [8]. Therefore, we need to study the high-frequency electrocardiogram (HF-ECG). Some studies have already found, that the HF-ECG measurements can provide a deeper look into the pathological state of the patient [8][14].

One way to study the HF-ECG is to extract the high frequency part of QRS-complex (HF-QRS) [8][15][14]. The main parts of HF-ECG can be found in the HF-QRS. This is because the HF-ECG has a significantly lower amplitude compared to the standard ECG [15]. This can be seen in figures 3 and 4.

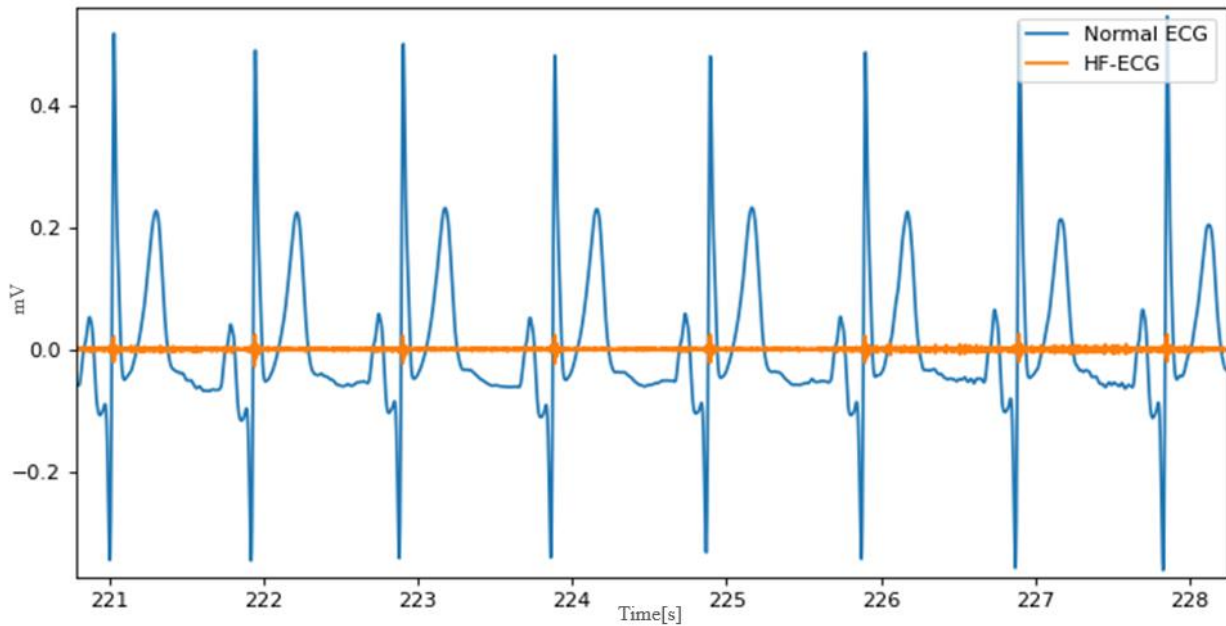


Figure 3. HF-ECG compared to the standard ECG from STAFF III.

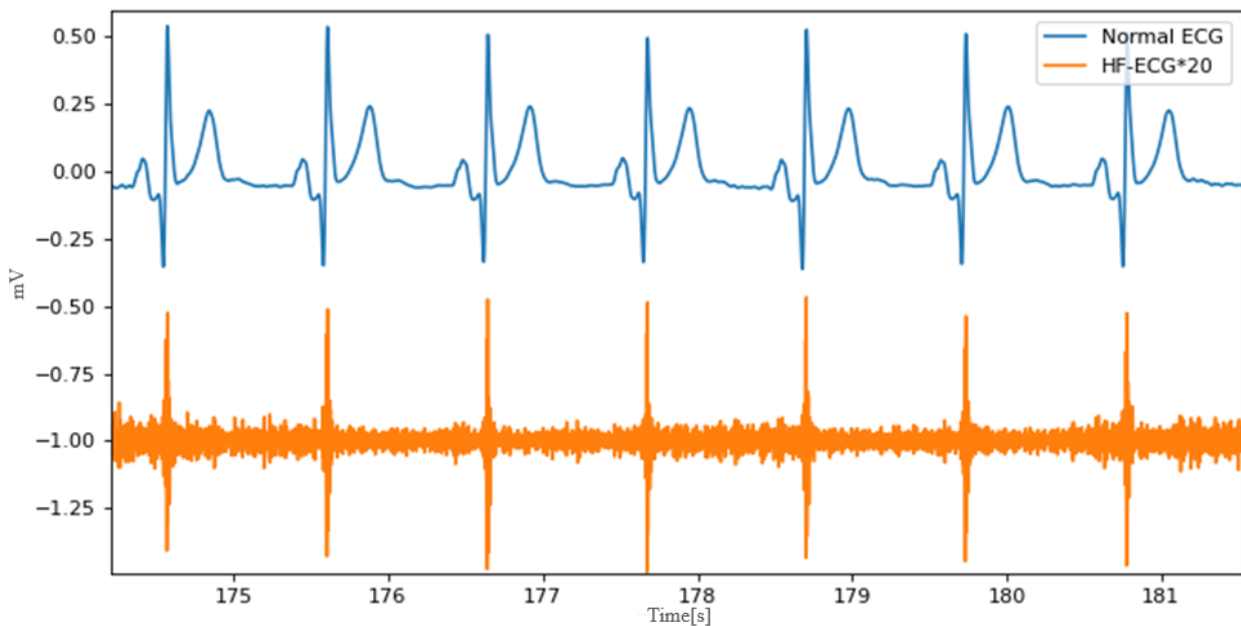


Figure 4. The same ECG and HF-ECG amplified by a factor of 20 and shifted downward -1.

Figure 3 demonstrates the difference in voltages in the different frequency ranges. HF-ECG has much lower amplitude and in figure 4 we can see that the only distinguishable features of the HF-ECG are the QRS-complex peaks. The HF-ECG in figure 3 has been amplified by a factor of 20 and has been filtered with high-pass filter of 150 Hz. Normal ECG is in the mV range, while the HF-ECG can be even in the μV range for some patients. Because the QRS-complex is the only clearly visible feature, most studies focus on the HF-QRS [8][15][14][16]. There is no established method to extract the HF-QRS, but most use signal averaging and bandpass filters [15]. These filters usually range from 150 to

250 Hz [8][15][16] and these are the frequency ranges where the HF-ECG studies have mainly been focusing. There have been some studies with lower frequencies as well, starting from 80 Hz, like myocardial infarction studies [28], but the most common bandwidth used is 150-250 Hz [8]. One way to study the HF-QRS is to compute the root-mean-square (RMS) from the signal [8][28]. Another method is to examine the shape of the HF-QRS [8][28]. The duration of the QRS is usually determined from the regular ECG and is then HF-QRS can be extracted from the HF-ECG [16]. If the patient is suffering from acute myocardial ischemia, from this HF-QRS envelope we can sometimes extract the reduced amplitude zone (RAZ) seen in the figure 5 [8][28].

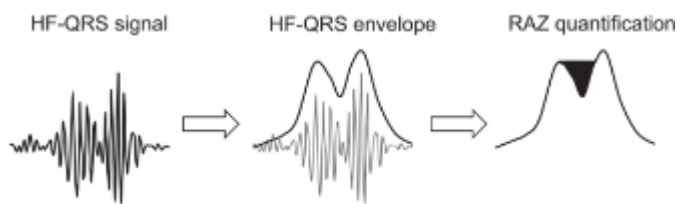


Figure 5. HF-QRS and RAZ qualification. Source: *Principles of Biomedical instrumentation* [28]

High frequency ST-segments can show some signs of ischemia or other myocardial diseases as well [28]. Ventricular late potentials (VLPs) that happen after the QRS-complex, can be seen in the HF-ECG. Some studies regarding to the P-wave of HF-ECG has also been made. K. Yodogawa et al. [30] found in 2012 that with high-frequency P-wave averaged signal, the difference between patients with and without atrial fibrillation can be seen from the HF-ECG. They filtered the signal between 40-300 Hz and averaged the ECG based on the P-wave. This shows that the HF-ECG has potential outside the HF-QRS.

The first published studies on HF-ECG was in the 1960s [15] and in 1980s first relevant results started to show up [8]. In 1980s multiple papers on HF-ECG was published, focusing mainly on HF-QRS [8]. Even though this was the case, HF-ECG has only recently gained popularity and commercial availability e.g. for diagnosing myocardial ischemia for example [15]. One reason for this could be because the physiological reasons for the HF-ECG are still unknown [14][16][28]. There are several theories trying to explain the changes in the HF-ECG and HF-QRS. Some believe that the HF-ECG demonstrates the conduction velocity and the fragmentation of the depolarization wave in the myocardium [16][28]. More physiological studies need to be done to determine the real physiological reasons for HF-ECG and changes in it [14]. Even though the physiological reasons for HF-ECG are unknown, the results cannot be disputed. Multiple studies have noticed the HF-ECG to be a relevant way to detect myocardial diseases [8][15][14][16][30]. Some studies even found out that the HF-ECG is more viable than the current methods [14]. One reason for the late bloom could also be that the HF

content has been found to be almost impossible to analyse manually [15]. Some studies have noticed that with leading edge technology, HF-ECG can provide a more detailed diagnostic [8]. With modern methods and machine learning, HF-ECG could be much more relevant than ever before.

The HF-ECG has been detected to have a high variability between the patients [14]. In my own studies I also noticed that the HF-ECG had much lower amplitude for some patients than others. This validates the type of study we want to execute. If the intervariability is high, the results from the straight up comparison can be distorted. Intraindividual variability might tell us more. Some studies have shown that for example the coronary artery occlusion can be detected easier with HF-ECG than the standard ECG [14]. These occlusions can lead to myocardial ischemia. One thing to note is that the normal ECG seems to be better at detecting the location of the occlusion, than the HF-ECG [14]. One reason for the detection was that the HF-QRS increased during the occlusion for some patients [14]. These results seem to support the fact that HF-ECG can be useful, especially for patients suffering from ischemic heart disease [16] and coronary occlusions [14].

2.2 Acute myocardial infarction

Acute myocardial infarction (AMI) is one of the main reasons of death all over the world [1][4][2]. AMI is more commonly known as a heart attack [1][31]. Usually AMI is detected in more developed countries, but nowadays it is also causing havoc in developing countries [4]. This is mostly due to unhealthy lifestyles. Over the last centuries, we have learned more and more about AMI and come up with new ways of treatment which have improved the rate of survival from the AMI [31]. Also the accuracy of AMI detection has risen over the years [1]. AMI can be defined in multiple different ways, depending on the field of study [1]. AMI refers to the cell death of cardiac myocytes caused by ischemia [1]. Ischemia on the other hand is caused by imbalance between supply and demand [1]. If the heart does not receive enough oxygenated blood for example, it will start to go to hypoperfusion. If this hypoperfusion is then prolonged, it will lead to ischemia which will then lead to the infarction when prolonged [31]. Simply defined, AMI is caused by decrease of blood flow to the heart causing to the cardiac cells to die [1][31]. AMI may also be the first sign of coronary artery disease [1].

One way to prevent AMI is by detecting myocardial ischemia. Ischemia can lead into structural damage to the cardiac muscle, rhythm disturbances and even to sudden cardiac death [8]. These are all factors when trying to predict AMI. It could be the first sign of coronary artery disease and could repeat itself [1]. Ischemia can be identified from the ECG recording of a patient [1]. Usually, also patient's myocardial history and lifestyle choices can be a factor when detecting AMI [1]. Detecting

AMI and ischemia from the ECG is not easy. Analysing the changes in the ST-segment is known to be a relevant method to detect ischemia [15]. The changes in the amplitude of the ST-segment are usually used to detect AMI and ischemia. AMIs which have these changes in the ECG are called the ST-elevation myocardial infarctions (STEMI) [4][31]. These kind of ischemic elevations could be the first signs of STEMI [5]. In STEMI, the ST-segments elevation rises drastically. This can be seen clearly in figures 2 and 6.

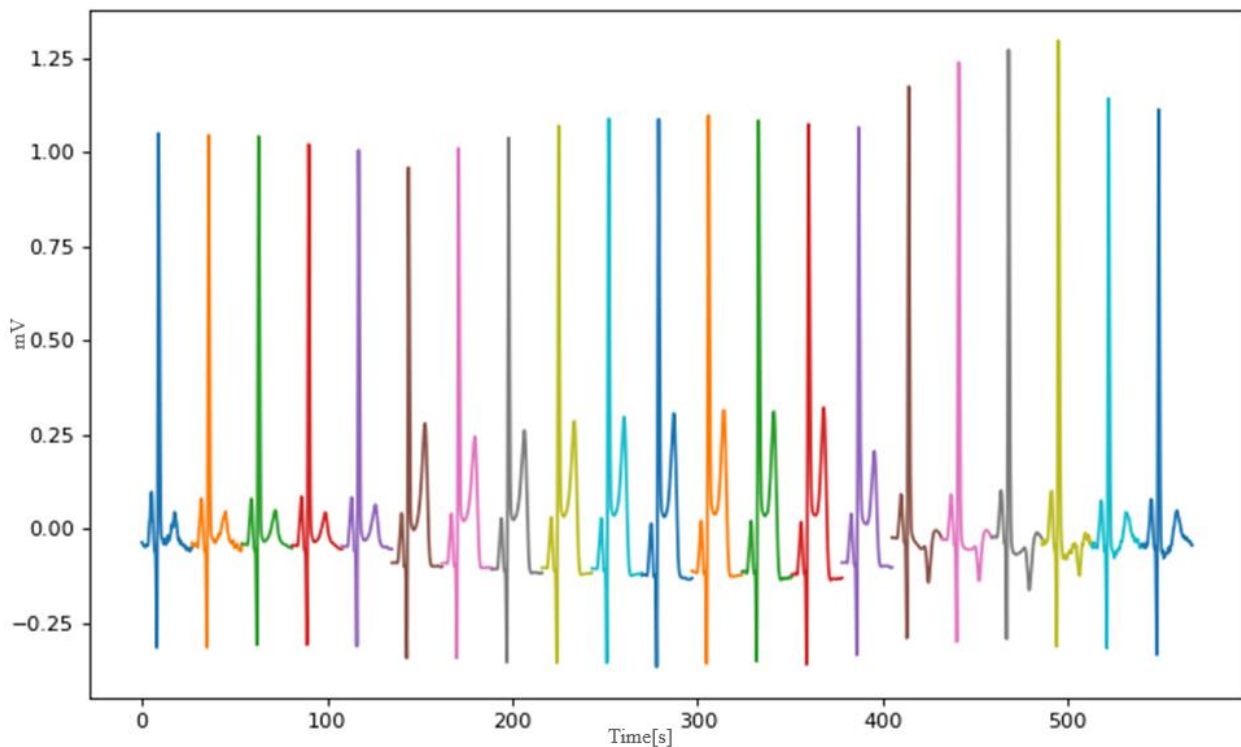


Figure 6. ST-elevation during AMI. The figure consists of average waveforms calculated every 30 seconds. Signal is from STAFF III database, recording 015c and lead II. Patient suffers from AMI.

Figure 6 demonstrates the changes in ST-elevation during AMI. The patient has been diagnosed to have an ischemia between 128-433 seconds [32]. In figure 6 we can clearly see the ST-elevation rise during the ischemia and then return to normal level of elevation after it. It has been estimated that over 3 million people every year suffer from STEMI [4]. Another huge problem is non-ST-elevation myocardial infarction (NSTEMI), which has been estimated to happen with over 4 million people every year [4]. In NSTEMI, the ST-elevation does not happen and it's harder to detect from the ECG [31].

ST-segments elevation is not the only sign of AMI in ECG. The PR-segment, QRS-complex and the T-waves can also show signs of AMI [1]. The R-peaks amplitude and changes in it, could be a sign

of AMI [1]. The width of the QRS-complex, especially if the segment between R- and S-peaks widen, could be a sign of AMI [1]. This is usually in correlation with ST-segments elevation. Also the spatial angle between QRS-complex and T-wave can detect ischemia [10]. If the T-wave appears inverted, it might be a sign of AMI [1][6], especially if ST-segments deviation shows signs of it [6]. The amplitude changes of PQ-segment can also be used to detect AMI [33].

After the AMI has happened, the ECG records may appear abnormal [13]. This is not always the case, and the ECG could be normal as well. Abnormalities in the ECG can occur, because the AMI has caused structural damage to the myocardial muscle [8]. These problems can further lead into rhythm disturbances and other problems which can lead to cardiac death [8]. Rhythm disturbances are caused by corrupted conduction factors and increased action potentials in the areas where the AMI has happened [13]. These changes can lead to abnormal electrical activity in the heart [13]. Most deaths with patients who have suffered STEMI or NSTEMI occur because of heart failure and structural complications like rupture somewhere in the myocardium [4]. Therefore, it is important to detect the AMI happening and then study the heart for possible problems. AMI usually leads to pain or discomfort which will last more than 20 minutes [1]. Other physiological symptoms may include shortness of breath, perspiration, nausea and even fainting [1]. These all should be a sign to go to the hospital. One problem is that people are hesitant and unsure when to go to the hospital. Another problem is that painless AMI, also called silent AMI, can occur [1][34][35][33]. Especially patients who are suffering from diabetes mellitus, are known experience painless AMI [34]. However, painless AMI has been noticed to occur with other patients as well [35]. Due to the structural damages caused by the infarction, it is crucial to detect also these silent AMIs. As stated, the ECG records can change after AMI, which is why regular ECG recordings are recommended [13]. Also during the AMI, even though there might not be any other signals of it, the ECG could be the only detection method [1]. Recording ECG continuously is probably not the answer though but predicting and preventing the possible AMI with regular ECG recordings could be. One thing to note is that the more we have understood the reasons behind AMI, the better we have been able to detect myocardial infarctions [1].

2.3 Available methods

There are multiple different methods on how to detect AMI. The 12-lead electrocardiogram is the golden standard when detecting AMI, but it is not easily accessible for the patients. It usually can't be measured at home by the patient. In this chapter we go through some potential competitors for our

device. Focus will be on portable devices, which the patient can use by himself. There has been an rising interest towards health technology and especially wearable devices in the recent years and COVID-19 pandemic seemed to boost this interest even more [36]. The main reason behind these portable devices in healthcare is to track patients' health. Additionally the purposes of especially portable ECG devices are to advance the diagnostic process [37] and to reduce time spend in doctor's office. It has been noted that the patients do not seem to struggle using these kind of technologies [36]. The fact that healthcare can be very expensive and that the cardiologist might not be available for every patient all the time, supports the need for self-used portable devices [38]. The financial savings could reach even billions with these kind of devices [38], while the devices themselves would have enormous financial opportunities.

2.3.1 AliveCor

AliveCor is a company from the United States that develops medical devices. They have multiple different products, but the focus is set on their latest device. This product is called KardiaMobile 6L. KardiaMobile 6L is an ECG device which can record up to 6-leads of high quality ECG [36]. The 6-leads include all six limb leads [36][39]. This means the I, II, III and aVL, aVF, aVR leads. The 6L has been given the validation by the United States Food and Drug Administration (FDA) to record ECGs [36][39]. The system consists of the ECG capturing device itself and also an application called KardiaStation developed by AliveCor [36]. The device is rectangle shaped and fits easily in a person's pocket. This means that it is conveniently portable and works anywhere [39]. After the recording, you can look at the ECGs yourself and also send them to your doctor for inspection [39]. The device is shown in figure 7.



Figure 7. 6-lead ECG with KardiaMobile 6L. [39]

The device works by placing the sensor to skin on your left leg and fingers from both of your hands. This is demonstrated in figure 7. Once activated, the device records a 30-second long of ECG [36]. The ECG recorded is sampled at 300 samples per second. This makes the study of high-frequency ECG possible, but not all that reliable since Nyquist's sampling theorem declares that the sampling rate should be at least two times higher than the highest frequency component of the signal [40]. This means that the highest possible frequency from KardiaMobile 6L is 150 Hz, which barely scratches the range of HF-ECG.

After the recording the ECG is then send via Bluetooth Low Energy to a mobile device for diagnostics [36]. AliveCor claims that they can automatically detect AF, bradycardia, and tachycardia. It also detects the normal heart rhythm. The results are ready within minutes [36]. Automatic AMI detection with the application is not available, but under development. However, when the patient is suffering with chest pain, they can record the ECG and then send it to a doctor to further analysis.

2.3.2 HeartBeam

HeartBeam is a medical device designed to detect AMI [41]. It's developed by a company named HeartBeam in the United States. The device is capable of recording 12-lead ECG [41], but the leads have to be recorded separately. The device itself is very similar to the KardiaMobile 6L, which was introduced in the last chapter. It's the size of a credit card and can be with the patient all the time. Contrary to the 6L, HeartBeam does not have FDA approval and it is not in the market yet. However, the development seems to be in a good phase which is why it is included here. The device can be seen in figure 8.

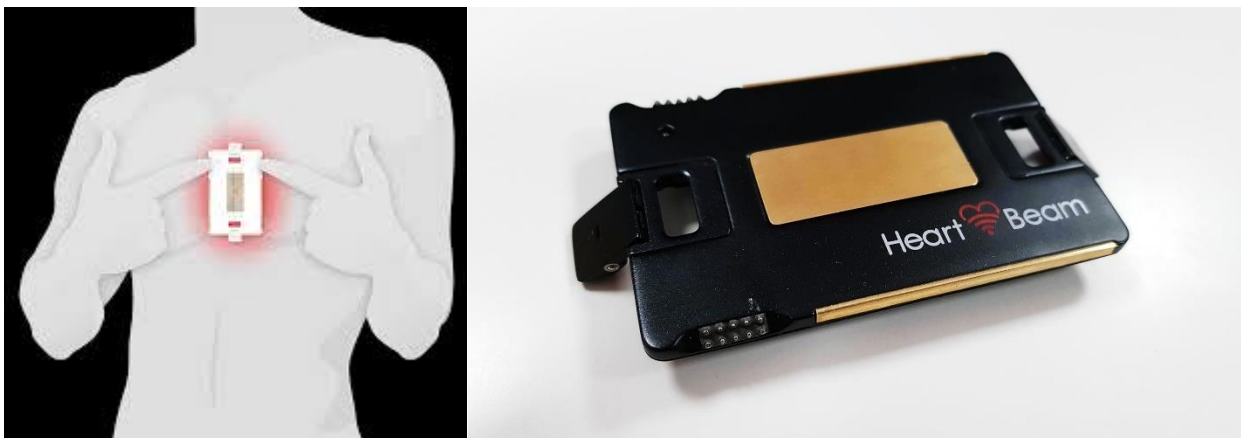


Figure 8. HeartBeam. [41][42]

This device can also be used by the patients at their home [41]. The ECG record can be done by placing the device on the chest of the patient and then pushing the sensors on the sides of the device with fingers from both hands. This is demonstrated in the figure 8. After the recording, the ECG is sent to a mobile device where the ECG can be evaluated in an application called iCardiologist. It is developed by HeartBeam and it sends the recorded ECG to a cloud where a doctor can access it and then can make the correct diagnosis [38]. They can determine if the chest pains are actually caused by an AMI or is it a false alarm [41][38]. The algorithms, sampling frequency and recording time of the device are not revealed by HeartBeam.

2.3.3 RELF Project

RELF Project is a medical project funded by Ghent University in Belgium [43]. RELF takes a little different approach to the ECG recording than the two previous. They have developed a handheld device that uses proper ECG electrodes rather than having them embedded in the device itself like in the two previous ones. The device is relatively small, and it and its leads on which the electrodes are attached to can be seen in figure 9.

The device seen in figure 9 is connected to a mobile device via Bluetooth [43]. For the mobile device they have created a user interface application where you can control the ECG device [43]. This application also analyses the ECG recordings. They have based the calculations on an automatic algorithm, called the RELF method, that they had been developing for 7 years before the publication in 2019 [43]. This algorithm has been proven to work very accurately at detecting ischaemia [44]. The results are then generated using this algorithm and automated feedback is given within 1 minute [43]. The algorithm uses ST-segments differences in the last 13 measurements done by the patient [43]. This takes advantage of serial-ECG and gives reliable results according to the study.

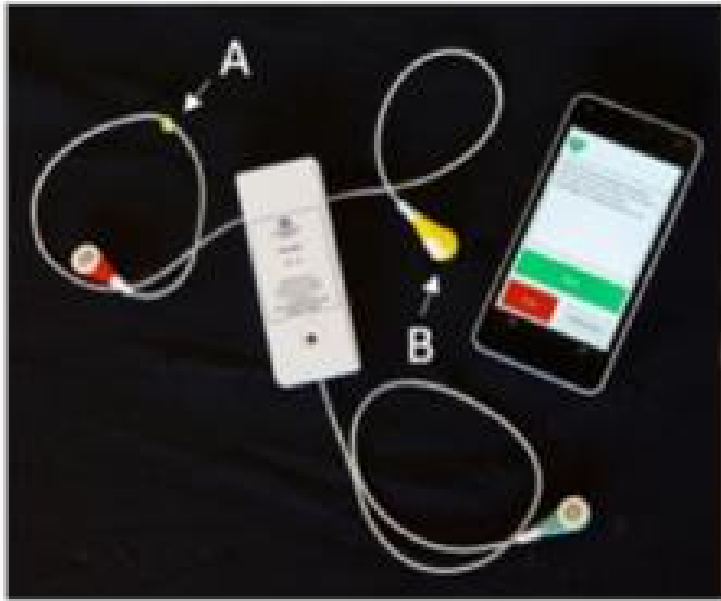


Figure 9. RELF device. [45]

They suggest that the patients should carry this device and electrodes with them and when experiencing symptoms should take the recording [43]. The recording itself is simple, the leads are connected to the right shoulder, left shoulder and to the left iliac crest located in the pelvic area [43]. The recording is 12 seconds long after which the mobile application tells you the analysis and adds the recording to the library. The sampling frequency of the recording is not revealed.

2.3.4 AngelMed

AngelMed Guardian System is a medical device system that alarms the patient about AMI. The system is made of an implantable medical device and an external device [33]. The implantable device is very similar to pacemaker and it provides continuous ECG monitoring [33][46]. The implantable device is planted on the patient's chest where it can detect myocardial changes [33]. The device will then analyse the ECG and if an abnormality emerges, it will alarm the patient via vibration [33]. In case the situation is severe, also the external device will start beeping and flashing to signal the patient to either call a doctor or an ambulance [33]. The alerting system is based on ST-segments changes [33]. Every 90 seconds the system records 10-second-long ECG and calculates the ST-segment values from it [33]. After the calculation, it will refer the values with 24-hour average of the patient [33]. If a reasonable ST level change happens, the device will then start to record ECG every 30 seconds [33] and if the trend continues, depending on the severity of the changes the device will warn the patient to go to see a doctor or alert an emergency [46]. Sampling frequency of the device is not revealed. In figure 10, we can see the external device and the implantable device.

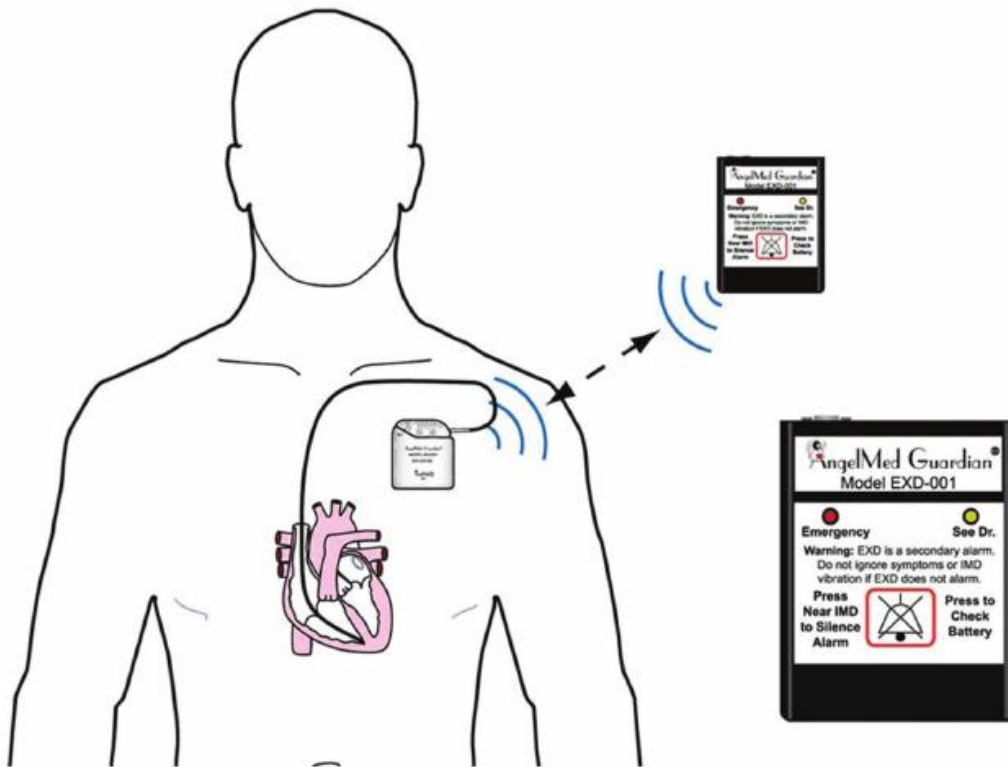


Figure 10. AngelMed Guardian System. [46]

2.3.5 Smartwatches

In the last few years, some smartwatches have been starting to provide the possibility to record ECG. One example of this is Apple's Apple Watch Series 4. This device has two electrodes, one on the back of the watch and one in the digital crown of the watch [47]. These two electrodes create a single-lead ECG, which can be used to acquire ECG from all 12-leads [48]. Apple Watch has been given the US Food and Drug Administration approval [48]. It has been mainly used to detect atrial fibrillation, but there are definitely possibilities to detect AMI [48]. It is important to note that the smartwatch is not meant for clinical tests [48]. However, it has been studied that the smartwatch can produce a signal that shows ST-segment and QRS-complex changes [48][49]. This can make the smartwatch an valuable asset when the standard ECG is not an option or available. The ECG signal from the watch is good enough for making tentative diagnosis and monitoring.

The ECG can be recorded in multiple different ways. The simplest way is to record Einthoven's lead I. If the patient is wearing the watch on his left wrist, as normally you would, then the recording can be done by placing your right index finger on the crown of the watch [49]. Other leads can be also recorded, but with different setups. One recording is 30 seconds long and the sampling frequency is not revealed. After the recording is done, the ECGs can be stored into Health Application made by Apple [47][50]. The application will then calculate and categorize the patient's ECG to normal

rhythm or some kind of irregularity [50]. The ECG is also visible for the users and it can be sent to a doctor if necessary [50]. One study found that when comparing these smartwatch ECG recordings to a 12-channel ECG, they both produced very similar signals [49]. In figure 11 we can see lead I being recorded.



Figure 11. ECG with Apple Watch Series 4. [47]

2.4 Machine learning methods

For the past decades, machine learning has been one of the most studied subjects in computer science [51]. Machine learning means that a computerized method can detect meaningful patterns from data [51]. Nowadays with big data, machine learning has become even more valuable. Some patterns can't be detected by humans, but with the right attributes machine learning can. This is why machine learning is widely used in different fields, including medicine and health technology [51]. In this study, we used 5 different machine learning methods. All of these methods are classification methods, which is a supervised machine learning technique [52]. Classification is one of the most used machine learning techniques [52]. In classification-based machine learning, the algorithm is first given a training set which has input and output values. In this study for example, input values are features gathered from the patient's ECG signals, while the outputs are the labels given for these patients. After the algorithm has been trained, then it can be given a test set with only the input values [52].

Then the algorithm tries to predict the output based on these inputs. It is called supervised machine learning because of the training sets given to the algorithm are all known [52]. The test and training set is usually split so that the training set includes 70-80% of the data, while the test set is the remaining part of the dataset. This way the results will be more relevant, and the training will be enough depending on the size of the dataset. All of the machine learning methods used in this thesis are presented in the following subchapters, and are created with scikit-learns machine learning library [53].

2.4.1 K-Nearest neighbors

K-nearest neighbors (KNN) is one of the simplest machine learning methods [51]. The way it works is that the model memorizes all of the training set and then classifies the test data instances based on reviewing the closest data points next to it [51]. The number of closest points or ‘neighbors’ is determined as the ‘k’. It can be changed to any value, but in binary classification it should be an odd number so that the prediction does not end in a draw. This all is based on the expectation that all things that look the same, must be the same [51]. The benefits of this method are that it is easily executable and also it calculates very fast even though if the data set is big [51]. Figure 12 shows this method in action.

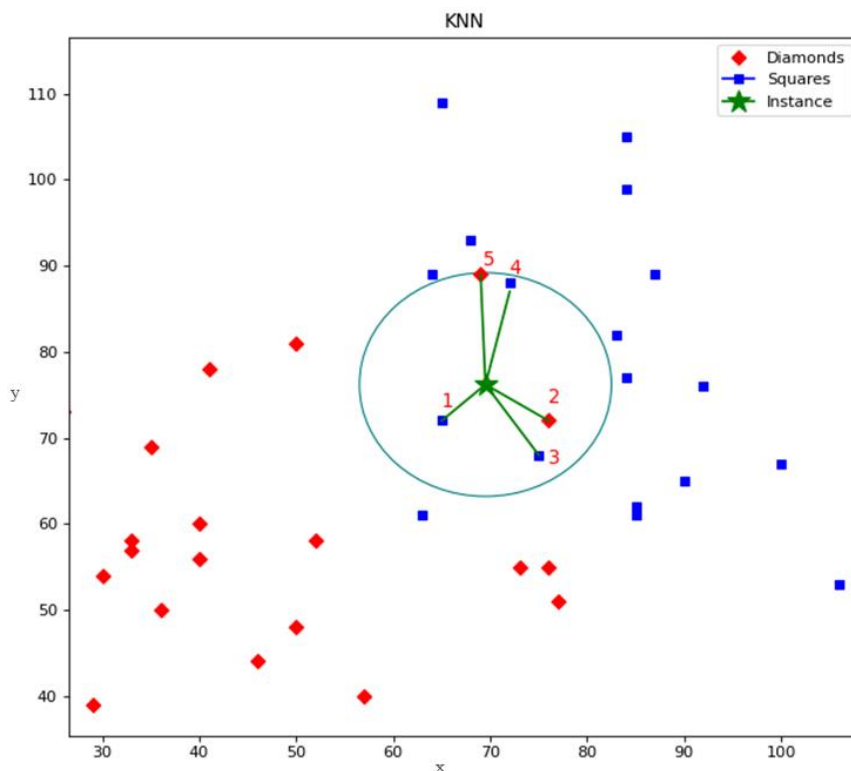


Figure 12. K-nearest neighbors machine learning method.

Figure 12 shows the nearest 5 neighbors of the instance. 2 of these neighbors are diamonds, while the other 3 are squares. This means that the green instance will be predicted as a square with KNN, if the k-value is 5.

2.4.2 Support Vector Machine

Support vector machine (SVM) is a supervised machine learning method where the goal is to divide the classes as well as possible with a hyperplane [52][54]. It has been determined as a great method at detecting heart diseases with relevant features [2]. SVM relies on statistical learning theory [52]. It can be used as a regression model, but support vector classification (SVC) model is used more often. Depending on how many features (n) the classes have, the SVC will create (n-1)-dimensional hyperplane to separate the classes. Maximising the separation between these classes is key when using SVC and reducing errors [52]. This separation can be seen in figure 13.

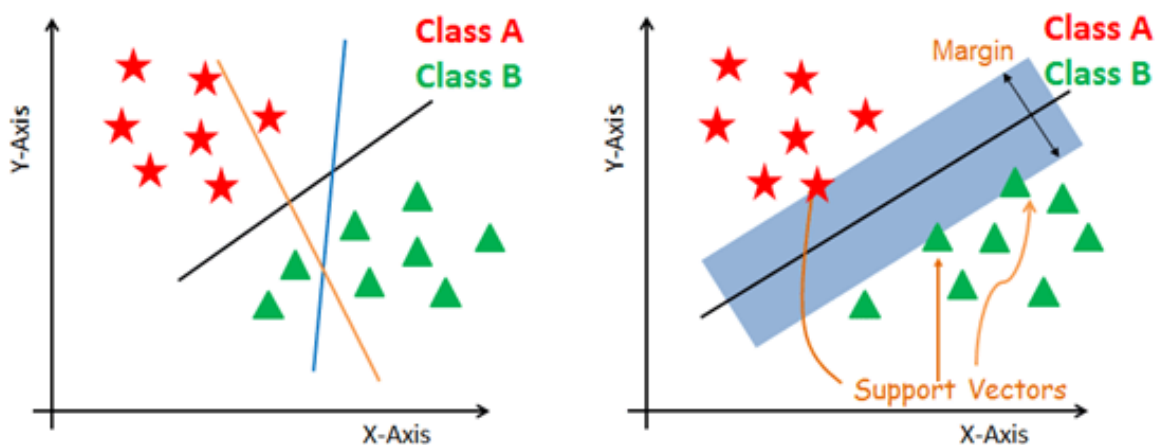


Figure 13. Support Vector Machine. [55]

Figure 13 represents the simplest form of SVC. In this SVC, there are only 2 features x and y, which means that the model has only 2 dimensions. The hyperplane then is simple line, which can be placed anywhere between the two distinct groups. The most optimal placement is exactly in the middle of the two groups, minimizing possible errors when predicting new values. This is represented by the black line. The placement can be calculated with the help of support vectors that can be seen in the figure 13. These vectors are the outermost values, nearest to the other class [56]. These also give the name SVM for this machine learning method [56].

2.4.3 Decision Tree

Decision tree is a supervised machine learning method [52]. It predicts the label of the data based by travelling a decision tree from its root node through every node until a leaf node is reached and the answer is given [51]. Node can be described as a crossing, a question which will guide the decision in one way or another. Leaf node can then be described as the last point, where there are no more nodes to go to. Meanwhile root node is the complete data set. At every node in this root-to-leaf process, the data is split based on the features of the data [51]. Each node is then a test on a feature, depending on the value, it will make a decision and move on to the next node [52]. These features can be numerical or of other types of requirements. A very simple binary-classification is presented in figure 14.

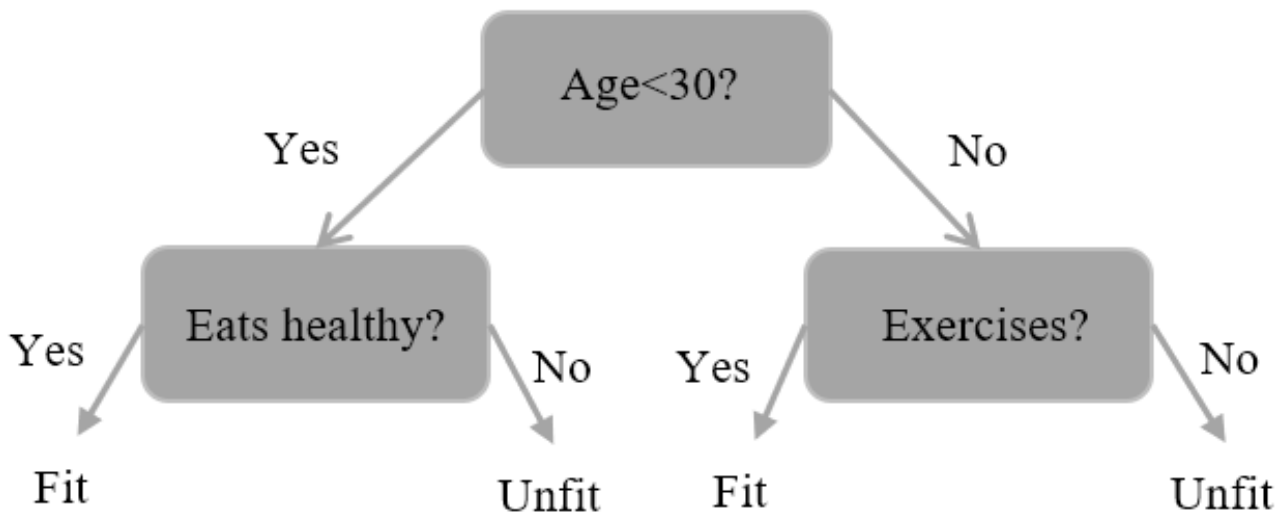


Figure 14. Decision tree.

Figure 14 demonstrates a really simple example of a decision tree trying to answer if the person is fit or unfit. The decision tree moves one question at a time and, based on the answer, moves on to the next question. After the decision tree has been processed, answer can be given.

Decision trees try to expose the structural information within the data [52]. If a human programmer makes a classifier, it usually works like a decision tree [51]. These methods are reasonably simple and fast, while having a good accuracy [52]. However, on a complex data this method might not work perfectly, since they are computationally hard to learn [51] and also some of the complexity can be overlooked by the simplicity of this method. Decision trees can also suffer from overfitting [51].

2.4.4 Random Forest

Random Forest is a supervised machine learning method, which consists of multiple decision trees [51]. It can be a classifier or a regressor. The way it works is that it uses multiple different decision trees and then with results of these trees it makes the predictions based on majority vote [51]. With this kind of machine learning, the method reduces the possibility of overfitting and also handle more complex data [51]. While using multiple decision trees to make a prediction, the computational complexity becomes much higher. This can limit the usage of this machine learning method in real-time solutions. Figure 15 demonstrates the usage of random forest classifier with 3 decision trees.

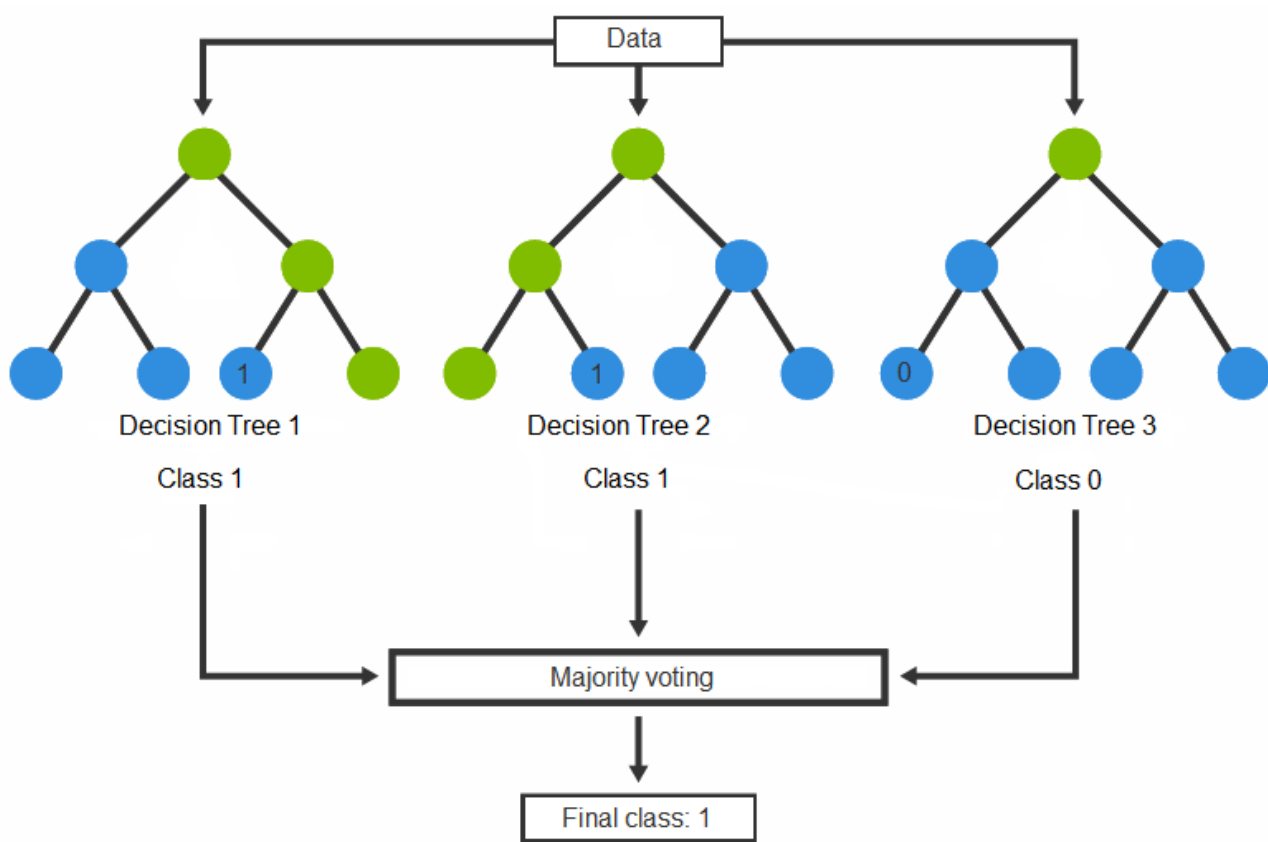


Figure 15. Random forest.

2.4.5 Extra Trees

Extra Trees is a supervised machine learning method, very similar to Random Forest. It uses multiple randomized decision trees and then makes a decision based on the majority vote. The main difference between Random Forest and Extra Trees is that, while Random Forest uses bootstrap replicas and

chooses the optimum split, Extra Trees randomizes the split and uses the whole sample [57]. Extra Trees algorithm is also computationally faster than the Random Forest [57], making it a good option.

2.5 Cross-validation

The machine learning models need to be trained. For this, the models need training data. The models also need to be tested, which also requires data, test data. If the dataset used is not big enough, it might affect the performance of the machine learning methods. To avoid this happening, one solution could be cross-validation [15]. Usually, the data is randomly split between training and test in the sizes of training set being 90% to 70% of the data and the test set containing 10% to 30% of the data [58]. In cross-validation however, the dataset is split into these sets' multiple times. For example, in leave-one-out cross-validation (LOOCV), the training set contains all but one instance of the dataset. The one instance remaining is then used for testing. This operation is then iterated throughout the dataset, so that every instance of the dataset is left out one time. This means that every instance is used for testing in each iteration alone, while the rest of the dataset is used for training. Then the results are calculated together. With this kind of approach, we can make the most of the amount of data available [15][58]. Figure 16 demonstrates how the LOOCV works.

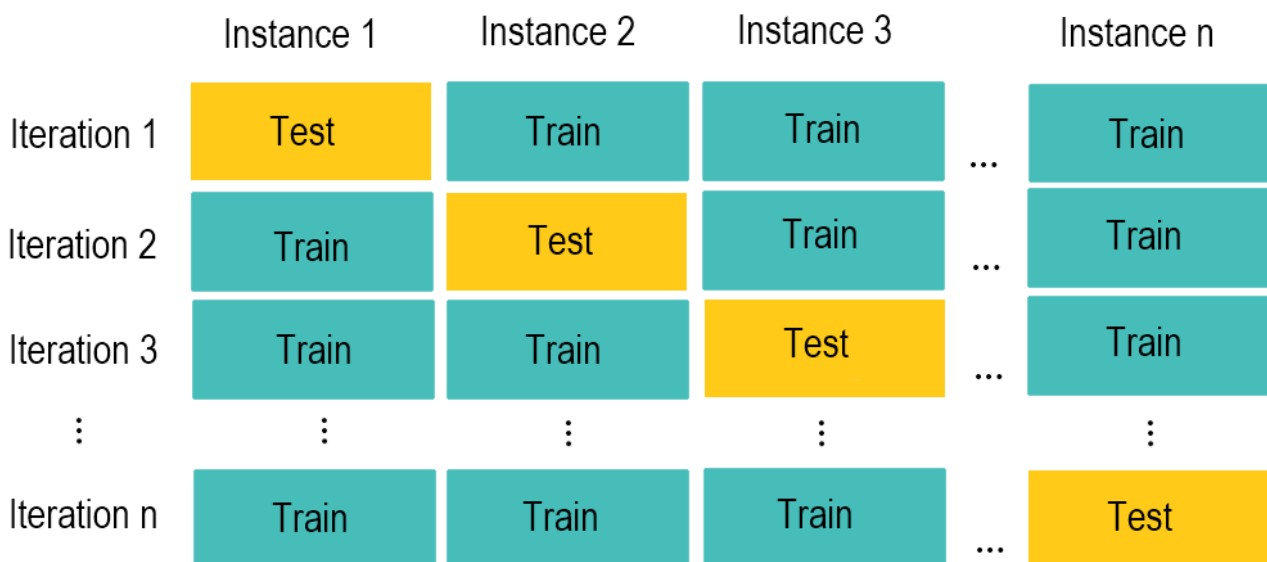


Figure 16. Leave-one-out Cross-validation.

3 STAFF III

3.1 Database

The STAFF III is a public database that was acquired to get a better understanding of ECG during acute myocardial ischemia [15][59]. It's a unique database since the AMI is caused purposely. This is possible due to prolonged angioplasty. Percutaneous transluminal coronary angioplasty (PTCA) was the method used [15], and it's a procedure where a blocking point or clot in the artery is opened. This method is the basic procedure after AMI [60]. This prolonged PTCA then causes the coronary artery to be blocked for some time, causing the ischemia to happen. The procedure of PTCA can be seen in figure 17. This is what makes the database special, they produce the AMI and record ECG simultaneously, which includes the full coronary occlusion.

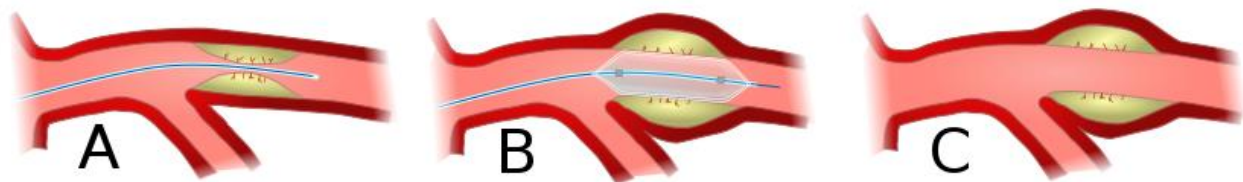


Figure 17. Percutaneous transluminal coronary angioplasty. Source: [61]

STAFF III was recorded in 1995-1996 in a medical centre in West Virginia, USA [15][32][59]. The ECG recorded was the standard 12-lead ECG [59], where precordial leads were placed with the standard placements, while the limb leads used Mason-Likar electrode placement in order to reduce noise [59]. Only voluntary patients receiving the PTCA were included [59]. The database includes 104 patients and all of these patients have multiple different ECG recordings [15][32][59]. These different ECG recordings include baseline data, balloon inflation data and post-inflation data. There are two different baselines: baseline 1 and baseline 2. Both are done pre-inflation. Baseline 1 is recorded in a relaxing room, where the patient is in a resting position [59]. This should be basically the best possible ECG that we can get from the patient. The recordings are 5 minutes long [59]. Baseline 2 is very similar to baseline 1, but instead of the relaxing room, it was done in the catherization laboratory [32]. It was also done in resting position and lasted for 5 minutes, but one

thing to note is that it was done right before the PTCA. This could mean that the ECG gets distorted due to nervousness or something else. This might affect the baseline 2 ECG, but it should still be very similar to the baseline 1. This is because the baseline 2 recording is done right before the inflation recording. Some patients do not have their baseline 1 ECG recording from the relaxing room, but instead it is done in the catheterization laboratory as well.

The inflation data was also recorded in the catheterization laboratory. These ECGs were acquired while the balloon inflation was applied to the patient [59]. Each patient have at least one inflation recording, but some patients have multiple balloon inflation recordings [59]. More than 2 recordings are rare, but one patient has 5 balloon inflations. The ECG recordings start before the occlusion happens and are carried on until the inflation is over. Unlike the baselines, the length of the inflation recordings varies a lot. Shortest recording is 1 min 30 s while the longest is 9 min 54 s [32]. The average time of the inflation recordings was 4 minutes and 23 seconds [32].

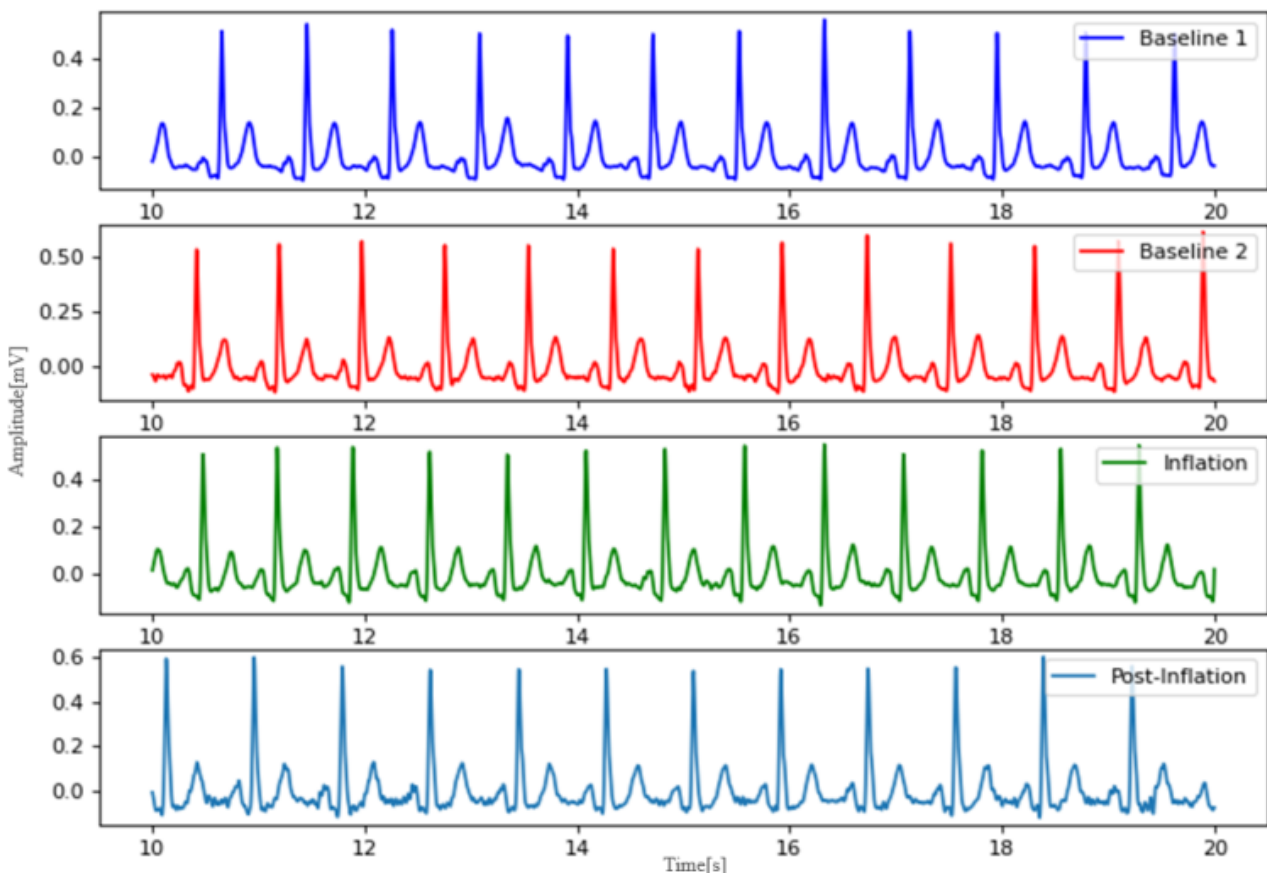


Figure 18. Different types of ECG recordings from STAFF III. Patient 102, lead II.

Patients also have post-inflation recordings. These ECGs are recorded after the PTCA is done and are done in a very similar way as the baseline recordings. There are two different kinds of post-inflation

recordings, ones done in catheterization laboratory while the other one is done in the relaxing room [59]. These recordings are 5 minutes long as well. In figure 18, we can see these different ECGs.

The full database can be found in physionet [32]. The database consists of *.dat and *.hea files [59]. They are marked from 001a to 108g. All of the patients have multiple recordings. Usually, A and B marked files are baselines, while c and further marked are inflations and post-inflations. Some recordings also have annotation files *.event to mark the balloon inflations and deflations [59]. The database also includes fully filled annotation Excel-file, which has a lot of important information regarding the database. The timings of the balloon inflations, the occluded arteries, age and sex of the patient and other important annotations can be found in this file. All of the annotations have been made manually [32]. This annotation file reveals that the database contains 152 balloon inflations in coronary arteries [59]. Of these, 58 happen in the left anterior descending artery (LAD), 59 in right coronary artery (RCA), 32 in left circumflex artery (LCX) and 3 in left main artery (LM) [59]. The annotation file also further divides these occlusions more specifically in the arteries, LAD for example is divided into proximal LAD, mid LAD, proximal mid LAD and LAD diagonal. However, more work has been done with ischemia detection from the data and the identification of the occluded artery has been mainly left out [15]. This is a bit of a mystery, because the site of the occlusion is known, so it would be easy to evaluate the efficiency of the identification method [15]. Some patients also had dye injections, which are also annotated in the annotation file [59]. These injections can cause some changes in the ECG [59]. However, all of the dye injections are not annotated so researchers analysing the database have to be cautious [59].

The STAFF III database also focuses on high-frequency ECG during ischemia [15]. This is the reason for sampling rate of 1000 Hz [59]. ECG also has amplitude resolution of 0.625 μ V [59]. These values provide high quality digital signals, which would show even the smallest changes that could be further analysed [59]. Although a lot of effort was put into it in order to record quality HF-ECG and it was one of the primary interest, there are no annotations made specifically for the HF-ECG content [15]. This is because the high frequency contents and changes are almost impossible to annotate manually [15].

Even though the STAFF III database is over 20 years old, studies are still done to this date [15]. Due to its unique nature with the prolonged PTCA and HF-ECG, it keeps on fascinating and providing new techniques for the researcher to study. The number of studies done with the database has only been increasing over the years, but most of the studies do not focus on HF-ECG [59]. It has been an excellent database to try new methods of detecting ischemia [15]. The database has also been

especially valuable when developing new or improving old signal processing methods [59]. The lack of HF-ECG studies done with STAFF III might suggest that it will keep increasing in popularity over the following years. The unique nature of the PTCA is also interesting. Usually the ischemic data is just brief inflation, but this database provides one long prolonged inflation [59]. This also could gain more popularity over the following years, since techniques providing ECG recordings from home already exist, but also in the future there might be a way of continuously recording ECG. This way we could get the full ischemia recorded from the patient in time and then compare it to this database's prolonged PTCA.

3.2 Comparing different ECGs

As stated, the STAFF III database consists of 104 patients, who all have multiple recordings from different kind of situations. In figure 17, we can see these different signals from one patient. It seems like that all the signals seem to be very similar to each other, at least with the first glance. When taking a more in-depth look, we can see that the post-inflation ECG seems to have more noise compared to the other signals. This might be due to the pain caused by the occlusion and then recovering from it. But the first three, baselines and inflation signals do not really tell a difference. We can evaluate the signals more closely by taking the average waveform of ECG based on the R-peaks detected from the signal. We can see these average waveforms in figure 19.

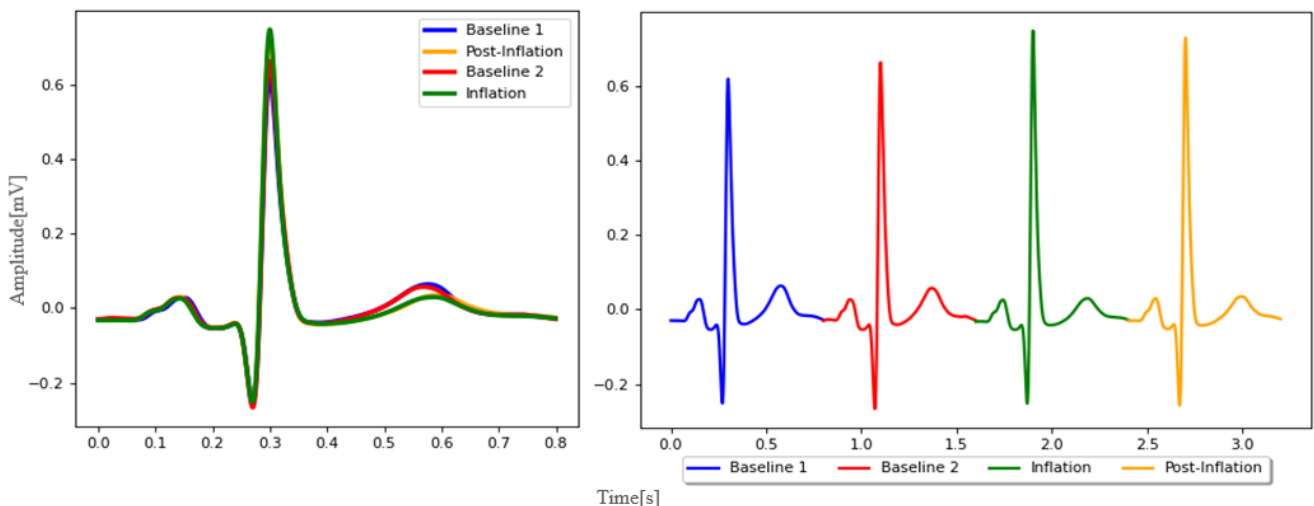


Figure 19. Average waveforms for the signals. From STAFF III database, patient 17 lead II.

In figure 19 we can see that even when comparing the signals in average waveforms, they seem to be similar. The most noticeable differences are in the height of T-wave and the R-peak. The inflation and post-inflation seem to have lower T-waves, but higher R-peaks than the baseline recordings.

Otherwise, they are almost equal. The form of the ECG, QRS-complex and the P-wave are all comparable to each other. One thing to note is that this is not the case for all the patients in the database, but this already gives us a lot of information regarding to the similarities between these signals. This provides us a great foundation to start comparing these different ECGs with each other and creating serial ECG analysis.

Baseline 1 and baseline 2 should always be very similar to each other, since they are recorded from the same patient, without any procedures yet to be done to the patient. However, there can be some changes due to nervousness and the basic nature of ECG. Also, the baseline 2 and inflation recording should be fairly similar, since they are recorded in the same room, in the same day and within minutes of each other. The inflation data of course has one artery occluded, but still the baseline 2 should be at least a little bit comparable with the inflation recordings.

For the serial electrocardiography analysis, we can then use two different types of comparisons. Baselines versus each other, and the baseline 2 versus the inflation recording. Basically, we will use the baseline 2 as sort of an anchor. The differences between baseline 1 and inflation recording are usually shown way clearer when compared in this way. Also, when using one ECG recording as an anchor, we should get more relevant results. This is basically what the S-ECG is about, comparing different ECG recordings with each other.

4 Signal processing

4.1 Pre-processing the data

As stated, the STAFF III database consists of *.dat files which are the signals. Each of these .dat files has a lot of information about the recording. The time of the recording, values of the analog to digital converter, information and comments about the patient and most importantly, 9 different channels of ECG. To read these signals, I have used waveform-database package [62]. This package makes reading and processing of the .dat files a lot easier. After reading the signal, I extract one channel of ECG and create timestamp for the signal based on the length and the sampling frequency of the signal. In figure 20 we can see an example of a full STAFF III ECG signal.

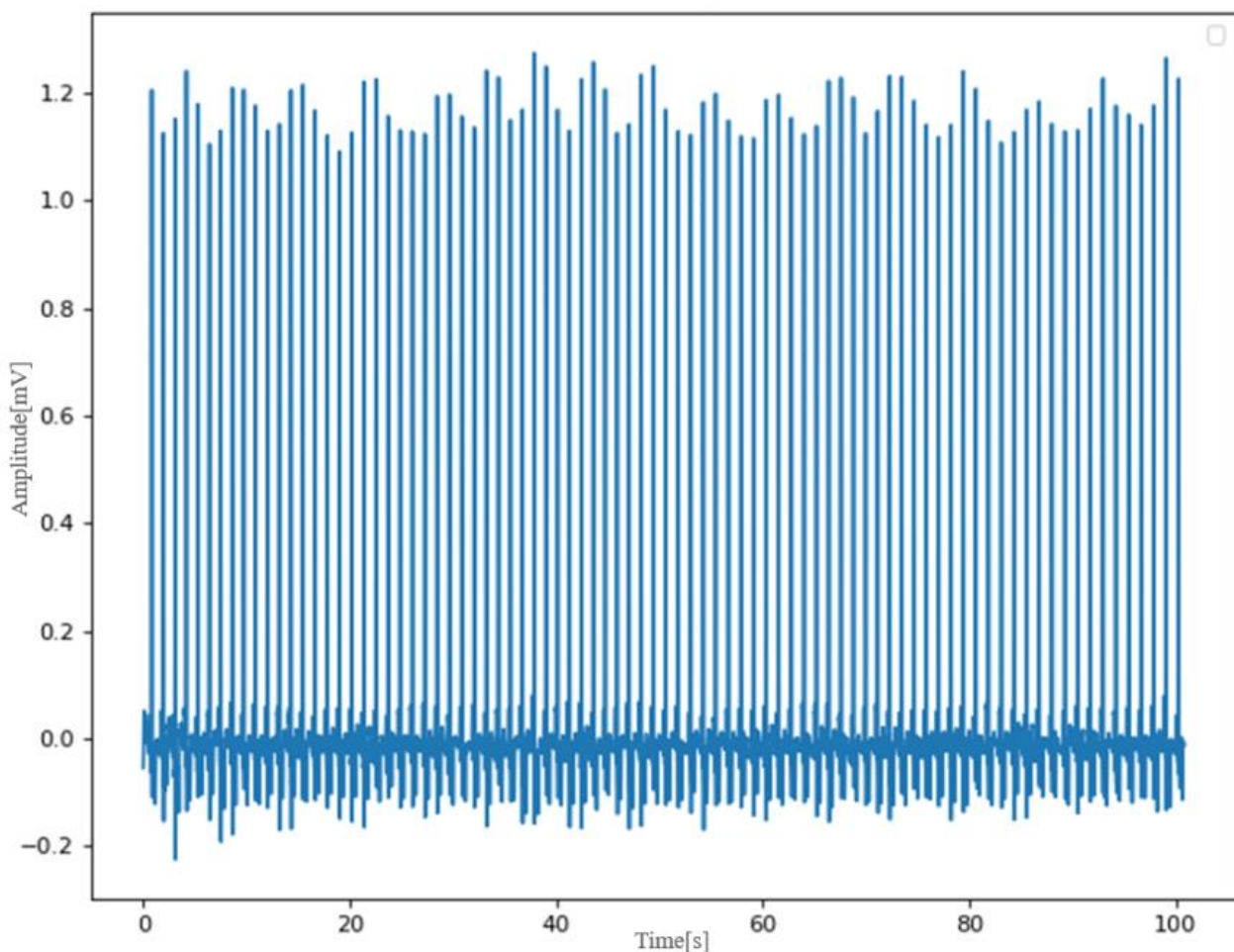


Figure 20. Raw ECG signal from STAFF III. Recording 45a, lead II.

Pre-processing process also included removing incorrect signals. Annotation file of STAFF III states that patients 1, 4, 5, 6 and 89 all have been identified as incorrect [32]. I did not include these patients in the study.

4.1.1 Filtering

The ECG signals were filtered to remove possible noise. The filtering method used for the ECG is Butterworth filter. I have used a bandpass filter with cut-off frequencies of 0.5 and 40 Hz. The filter is second order. For the high-frequency signal, I have used a second order high-pass Butterworth filter with high-pass of 150 Hz. The effect of these filters to the signal can be seen in figure 21. These cut-off frequencies are based on the literature considered in chapter 2. In some patients the HF-ECG might be stronger than others. This can be seen in figures 21 and 22.

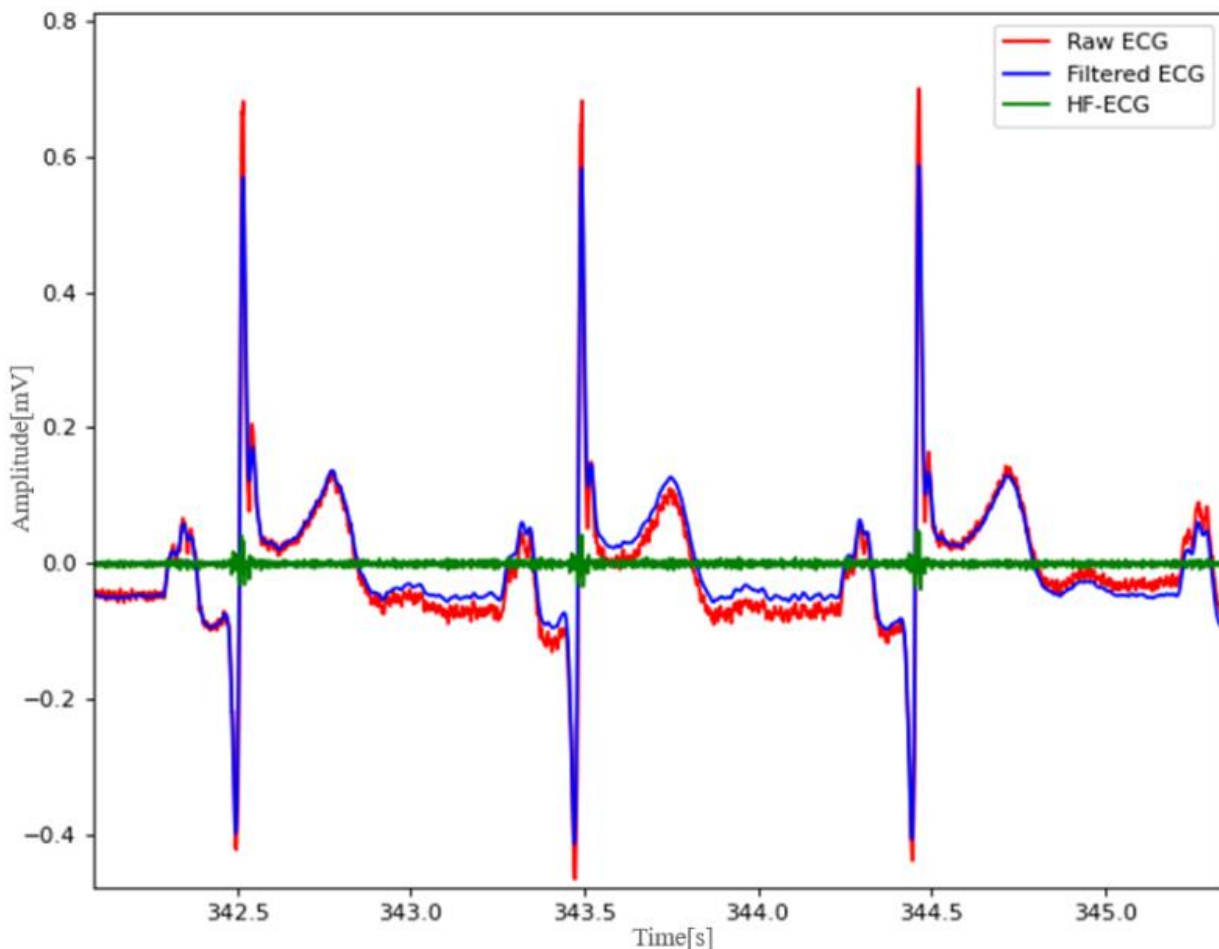


Figure 21. Raw, filtered and HF-ECG. From STAFF III, recording 17a, lead II.

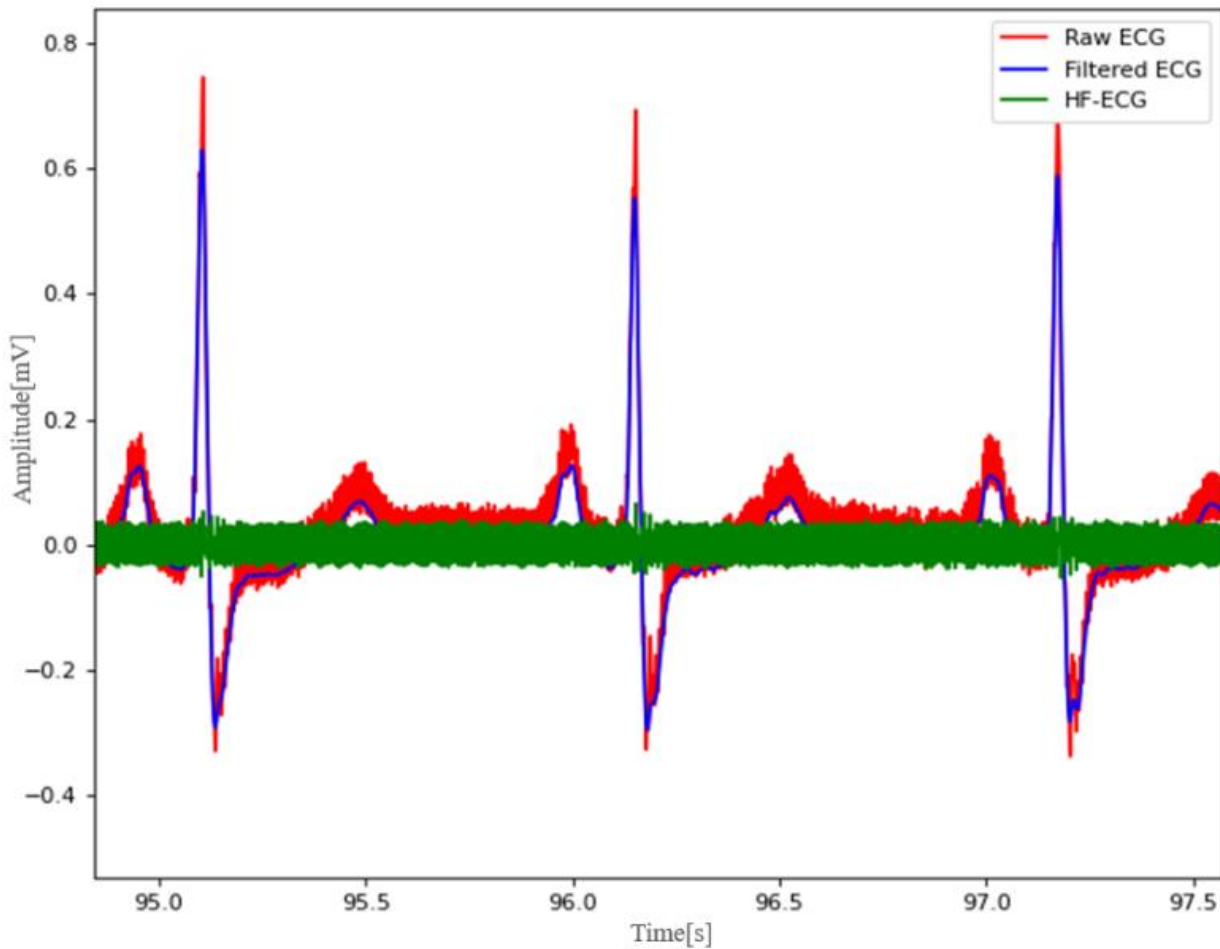


Figure 22. Raw, filtered and HF-ECG. From STAFF III, recording 32a, lead II.

4.1.2 Normalization

In order to make the ECG signals to appear more similar and reduce the possible intraindividual difference, normalization has to be done. Patients respiration can cause the ECGs baseline to drift, which can further change the nature of ECGs amplitude [63]. This can be reduced with normalization of the signal. Basically, it means scaling the signals to identical level. In this case, the signals are scaled from 0 to 1. This also means that the signals can't be negative [64]. Normalization is especially necessary when comparing ECG signals from different sources. The amplitude can change due to the equipment. The formula used to normalize the ECG is the following:

$$n = \sum_0^i \frac{x_i - \min(x)}{\max(x) - \min(x)}$$

where n is the normalized signal, x is the original signal and i represents the variable within the signal. The effect of this can be seen in figure 23. The signal itself does not change; amplitude of the signal

just gets altered. This way all of the signals will have the same power level. This needs to be done in order to compare the signals in respect to each other.

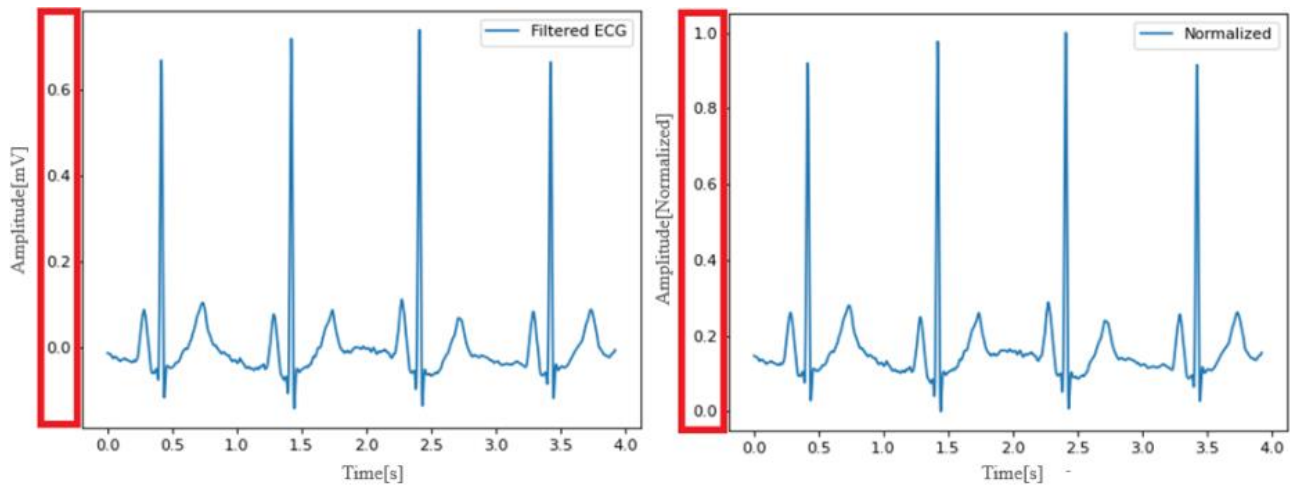


Figure 23. Normalization of the ECG. From STAFF III, recording 104a, lead II.

4.2 Peak detection

Peak detection can get interfered by noise [24]. Due to this, peak detection process can be started only after the signal has been pre-processed and filtered. STAFF III database does not recommend any specific nor include any peak detection methods [15]. We will want to detect the QRS-complex and the P- and T-waves. QRS-complex and R-peak detection is the most important thing in ECG processing and analysis [24][65]. Detecting the T- and P-waves of the signal is also necessary, in order to provide ST- and PQ-segment analysis [65]. Detecting these features helps us calculating features on which we can analyse and determine the patients' health. ECG is a periodic signal [23], which means that the P-, QRS-, T-wave cycles happens regularly and that the same peak detection methods can be applied throughout the whole ECG for all of the peaks. Most QRS detection algorithms already reach almost a 100% accuracy when detecting R-peaks [23], but noise and motion artefacts can be a problem. Also the speed, reliability and computational consumption varies within the peak detection algorithms [23].

4.2.1 R-peak detection

Over the years, multiple different R-peak detection algorithms have been established [24]. There isn't any generally accepted method yet [24], which means there is still room for improvement. This is one of the reasons why in this study we created our own R-peak detection method.

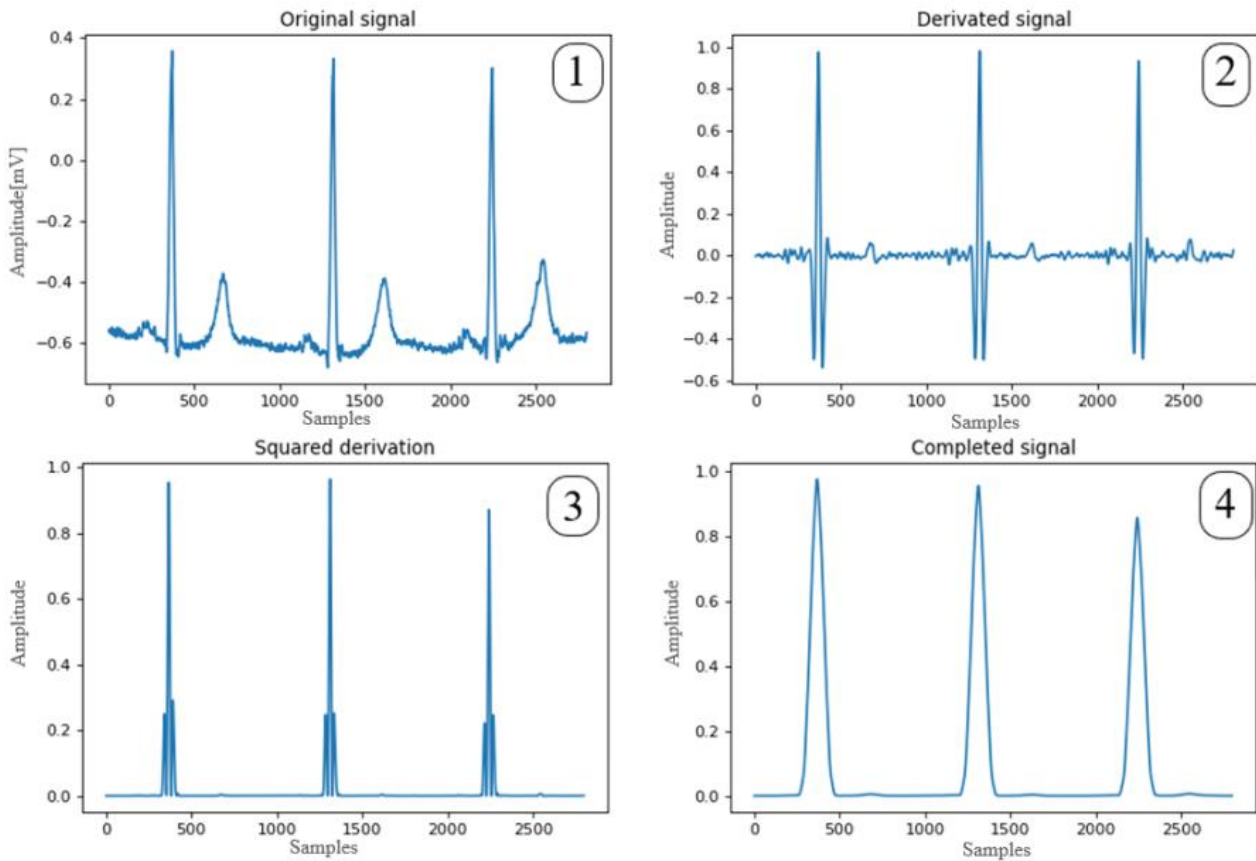


Figure 24. Processing the signal for peak detection.

In figure 24 we can see the process of breaking down the signal into peaks only. Some studies have proven that the R-peak is always positive [23] in some leads. One of the most noticeable features of the QRS-complex is its intense slope. By this I mean that the increase from Q-peak to R-peak happens suddenly and also the drop from R-peak to S-peak is rapid. This means, that the derivation around QRS-complex should be noticeable. And that was the first step, derivate the original signal in order to produce more clearly distinguishable R-peaks. This change happens in figure 23 from window 1 to window 2. After the derivation, the signal is squared. This is so that the signals derivation always is positive and shows the peaks once again more clearly. This happens from window 2 to window 3. After squaring the derivative signal, the signal gets integrated to produce only one peak per QRS-complex. After this, the signal is normalized by dividing the signal with its maximum value. This process can be seen from window 3 to window 4.

After the signal shown in window 4 of figure 24, it is very easy to detect the peaks. For this, SciPy's signal library's "find_peaks" method is used [66]. This algorithm requires parameters and based on those, it will return an array of peaks detected from the signal. The parameters include the signal itself and voluntary parameters like minimum distance between the peaks and the minimum required height

of the peak. For the distance I used the frequency of the signal divided by 4. The reason for this is because this would equal 0.25 seconds, which equals the heart rate of 240 BPM. This heart rate is not impossible for humans, but very rare. Also, in this database the patients are all in resting position and even though they are receiving PTCA, they should not have HR of more than 240 BPM. The threshold for the height is based on the mean of the processed signal. From the processed signal, we calculate the mean and then multiply it by 1.5. This threshold value should get all the weaker R-peaks from the signal as well. In figure 25, we can see the signal produced by the aforementioned methods, filtered signal and, in red, R-peaks generated by the detection method.

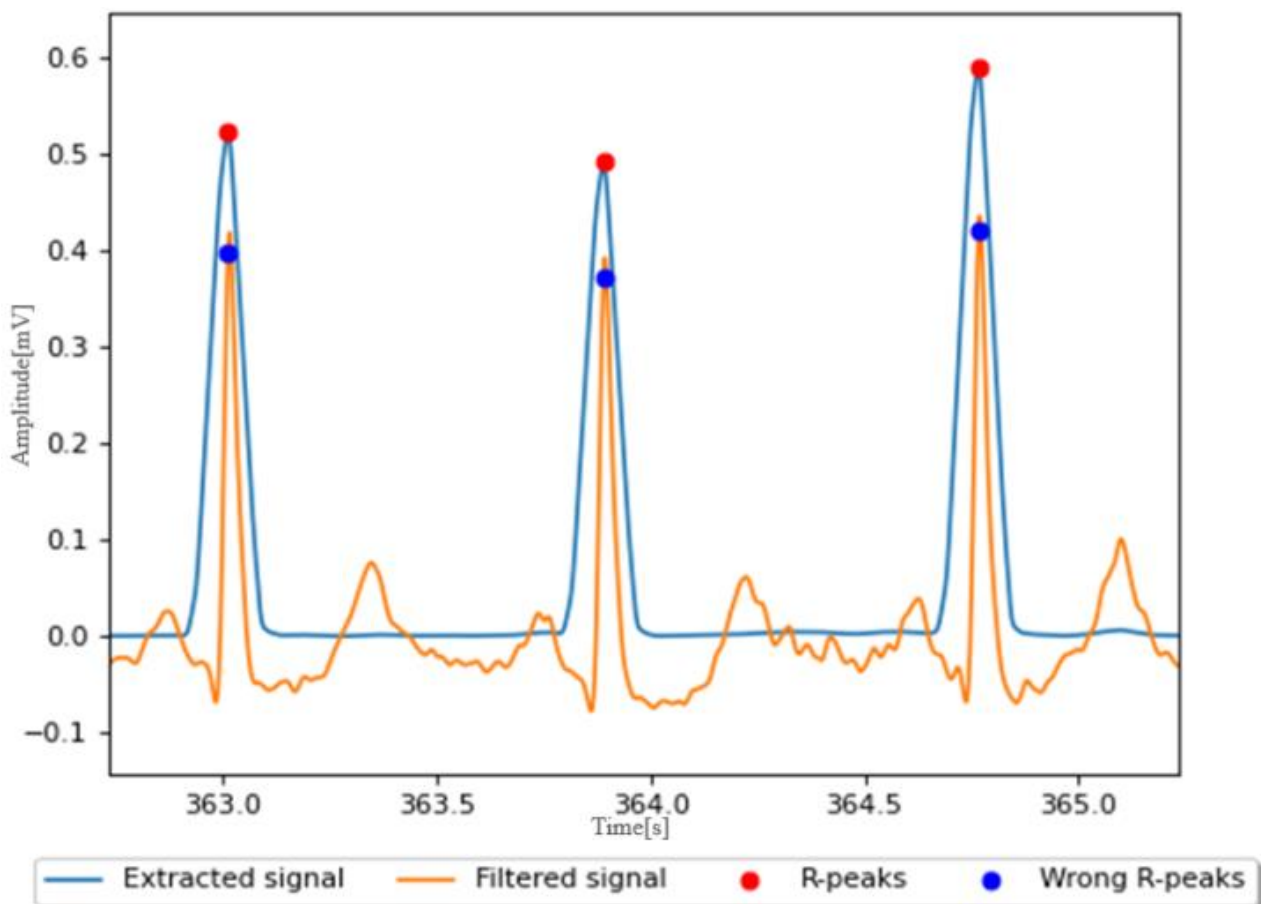


Figure 25. R-peak detection.

In figure 25 we can see that the peaks in the filtered signal (blue peaks) are a bit off. This is because these peak locations are taken straight from the extracted signal. To fix this, the correct peaks will have to be calculated. To do this, a window based on the extracted peak locations is created. The window includes an area of 0.1 seconds on both sides of the extracted peaks. Then the algorithm will

find the maximum value within this window. This will be the correct R-peak, which will be returned as an array of values of locations. The correction made can be seen in figure 26.

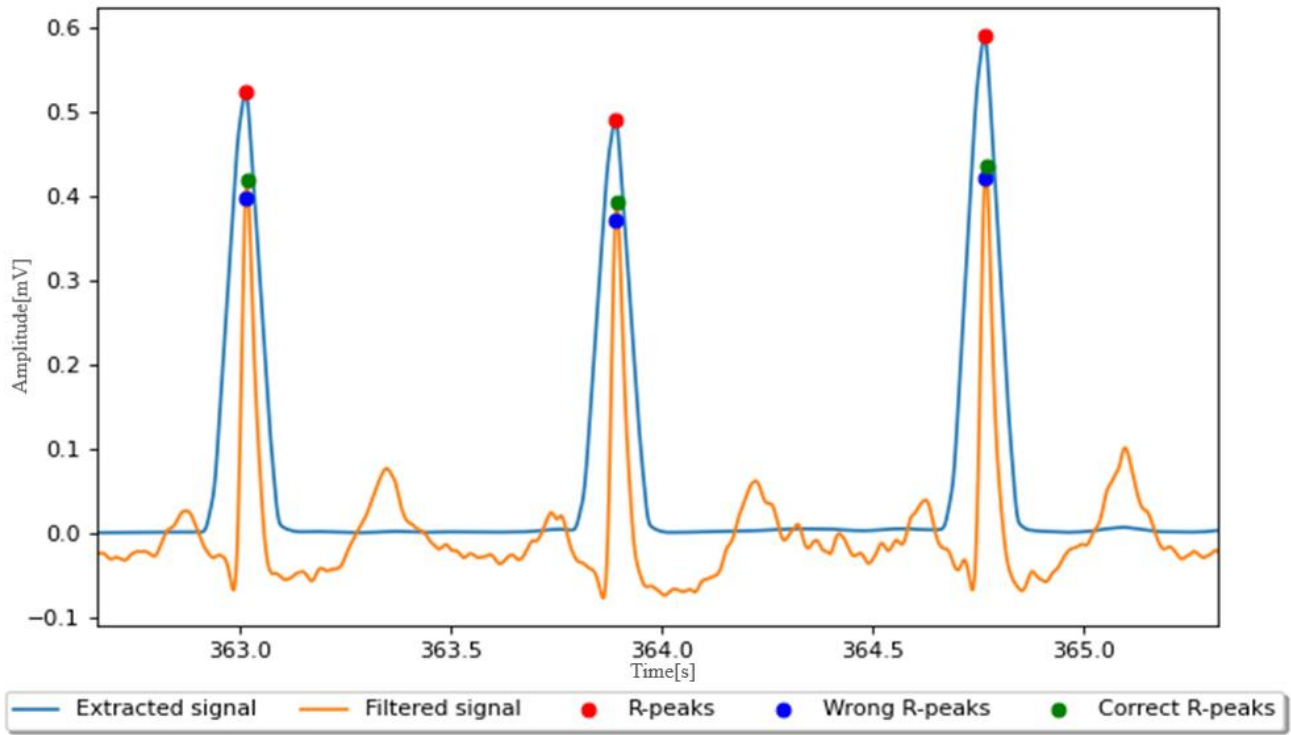


Figure 26. Corrected R-peaks.

4.2.2 P-, Q-, S- and T-wave detection

The P-, Q-, S- and T-waves are all important parts of ECG analysis. Detection method for these waves works based on the R-peaks we have identified with the previously introduced algorithm.

The P-wave is detected based on the R-peak. The algorithm creates a window before the R-peak and then locates the max value within this window. This should be the P-wave if the window is calculated correctly. The way the size and timing of the window is calculated is also based on the R-peaks. The mean difference between the peaks (RR-interval) is calculated and then based on the difference, a window is created. This window starts around $3/4^{\text{th}}$ of the gap between the R-peaks and ends $1/9^{\text{th}}$ before the next R-peak. From this window, we try to find the maximum value, which would be the P-peak. This is demonstrated in figure 27.

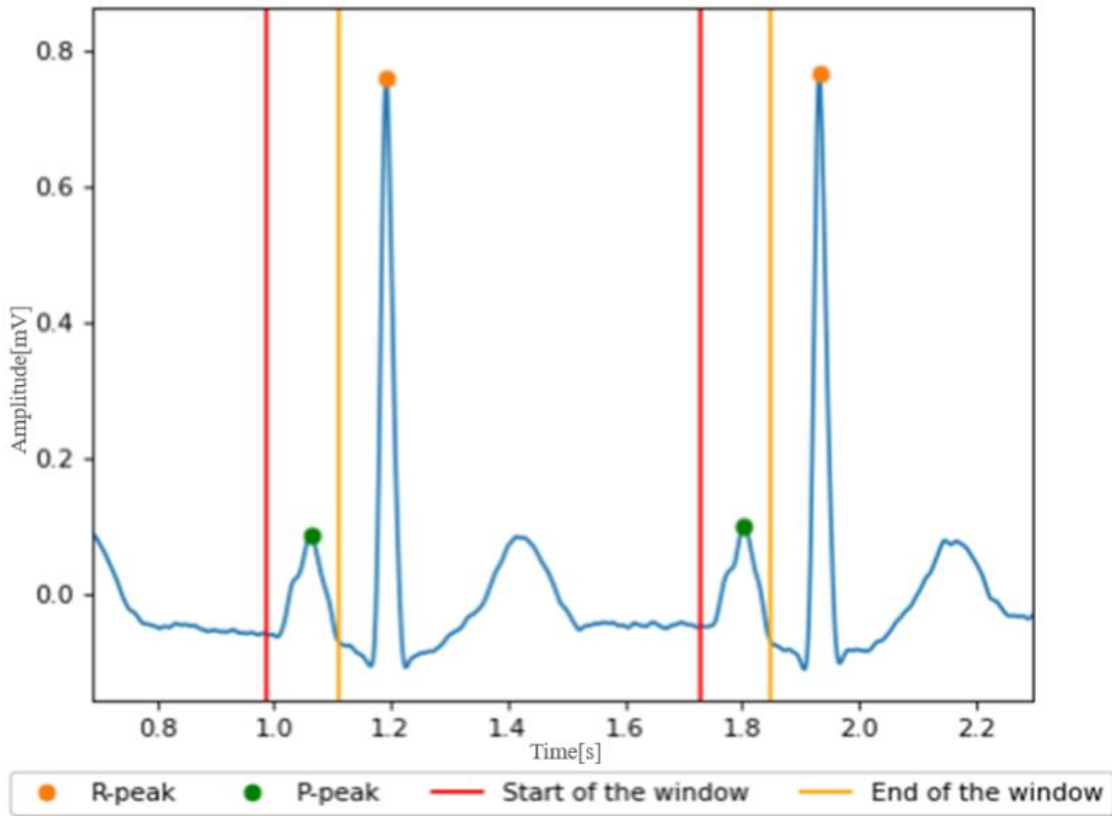


Figure 27. Detection of the P-wave. From STAFF III database, recording 48a lead II.

Figure 27 demonstrates the detection method for P-wave. Red line represents the starting point of the window, yellow line the ending point. Within these lines the algorithm finds the maximum value and returns it. Q- and S- and T-waves are detected based on the same method. A window is created next to the R-peak and then the peaks are detected. For every peak, the algorithm is a bit different. For Q-wave, algorithm creates a window between $15/16^{\text{th}}$ of the RR-interval and the R-peak itself. Within this window, it finds the minimum value. For S-peak the window is the same but starting from the R-peak and ending $1/16^{\text{th}}$ of the RR-interval, the algorithm finds minimum value within this window. These are demonstrated in figure 28.

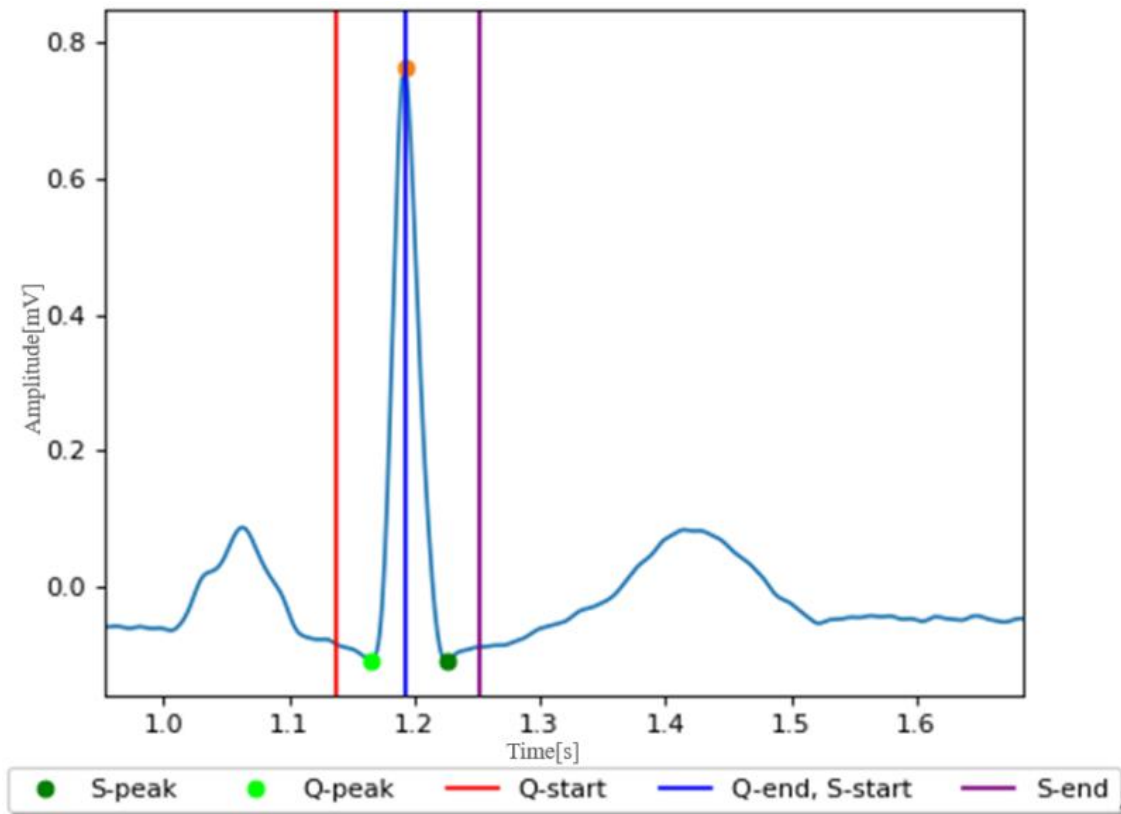


Figure 28. Q- and S-peak detection. From STAFF III database, recording 48a lead II.

The T-wave detection is done in similar fashion as the ones before. The RR-interval of the signal is calculated and then a window based on these values is created. The window starts from $2/9^{\text{th}}$ of the interval and ends at $4/9^{\text{th}}$ of the interval. Maximum value within this window is then found. This can be seen in figure 29.

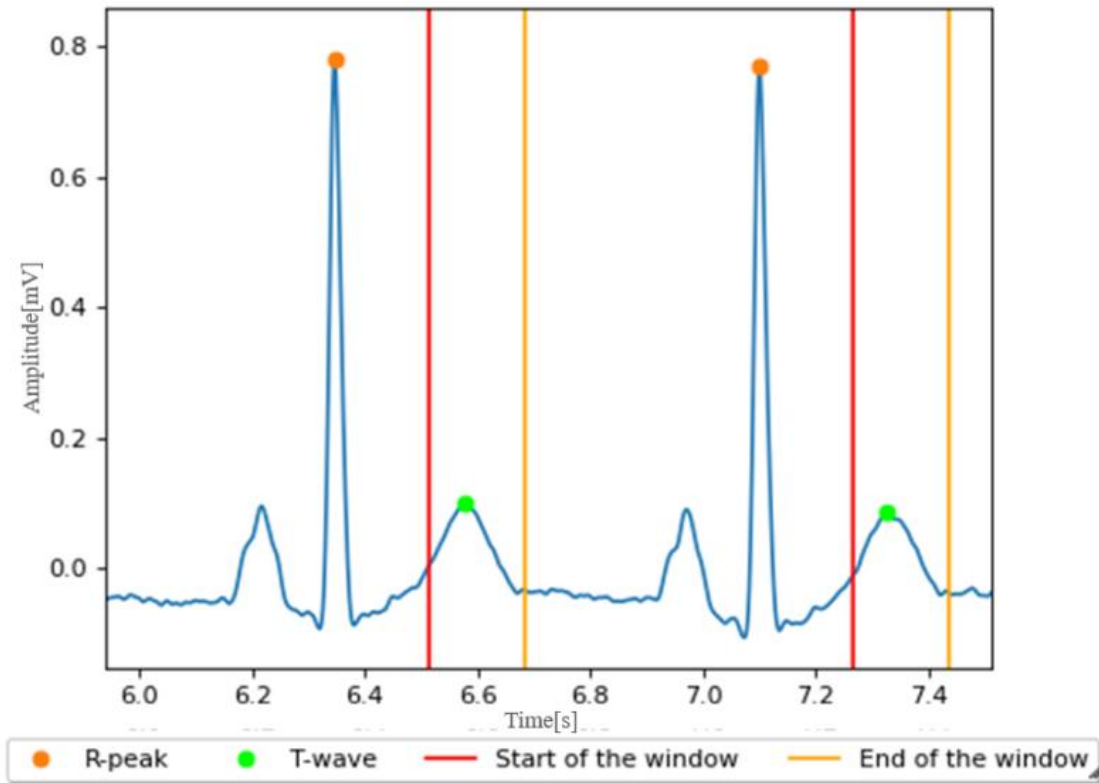


Figure 29. Detection of the T-wave. From STAFF III database, recording 48a lead II.

Figure 30 shows the ECG signal with all of the peaks detected.

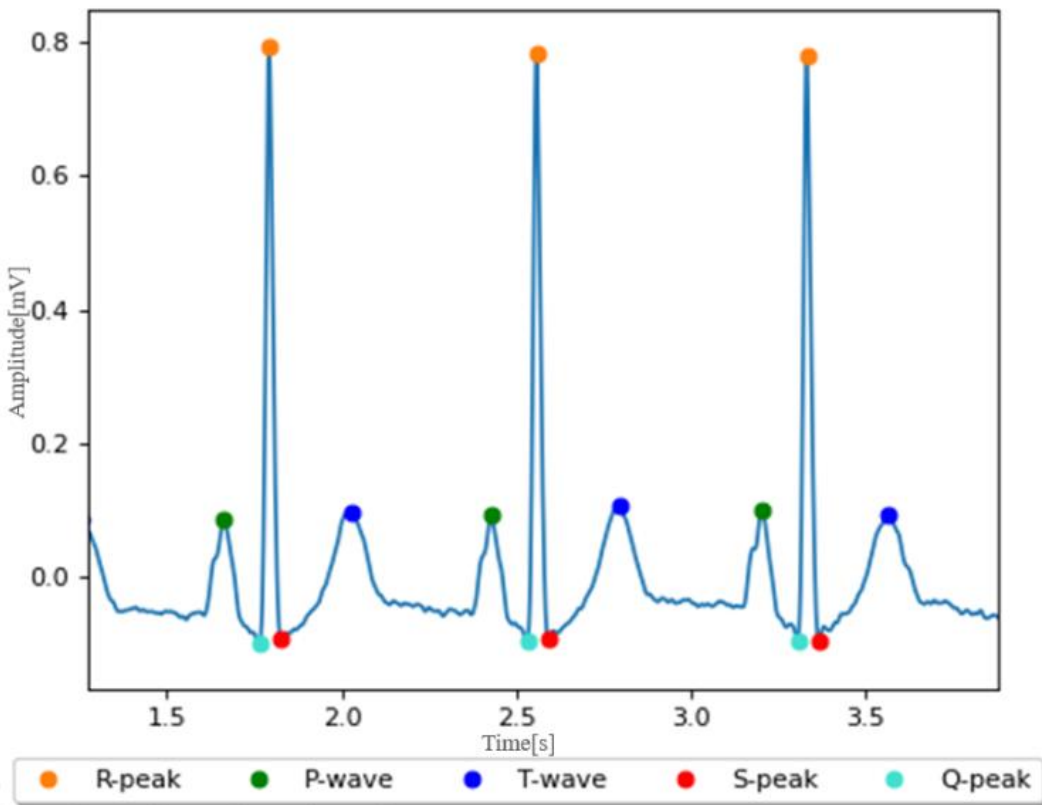


Figure 30. ECG signal with all the peaks detected. From STAFF III database, recording 48a lead II.

4.3 Average waveform

Average waveform is a method where the cardiac cycle of a full ECG recording has been averaged into one waveform. Since ECG is almost perfectly repetitive signal [23], averaging it is possible [67]. Motivation for waveform averaging is that it will improve the signal-to-noise ratio [67] and can possibly help to detect myocardial diseases [30]. Averaging needs to be locked to a point which is not based on time, but rather an identical reference point for all of the signal [67]. For this the R-peak is ideal since it can be easily detected and is also a vital part of the ECG analysis. Based on the R-peaks, the algorithm creates a window around the peaks and extracts this waveform created by the window to a list. After every waveform of R-peaks have been added, algorithm calculates the average of these waveforms. This can be seen in figure 31. The thick red line represents the average waveform, while the thinner lines all represent one single ECG waveform.

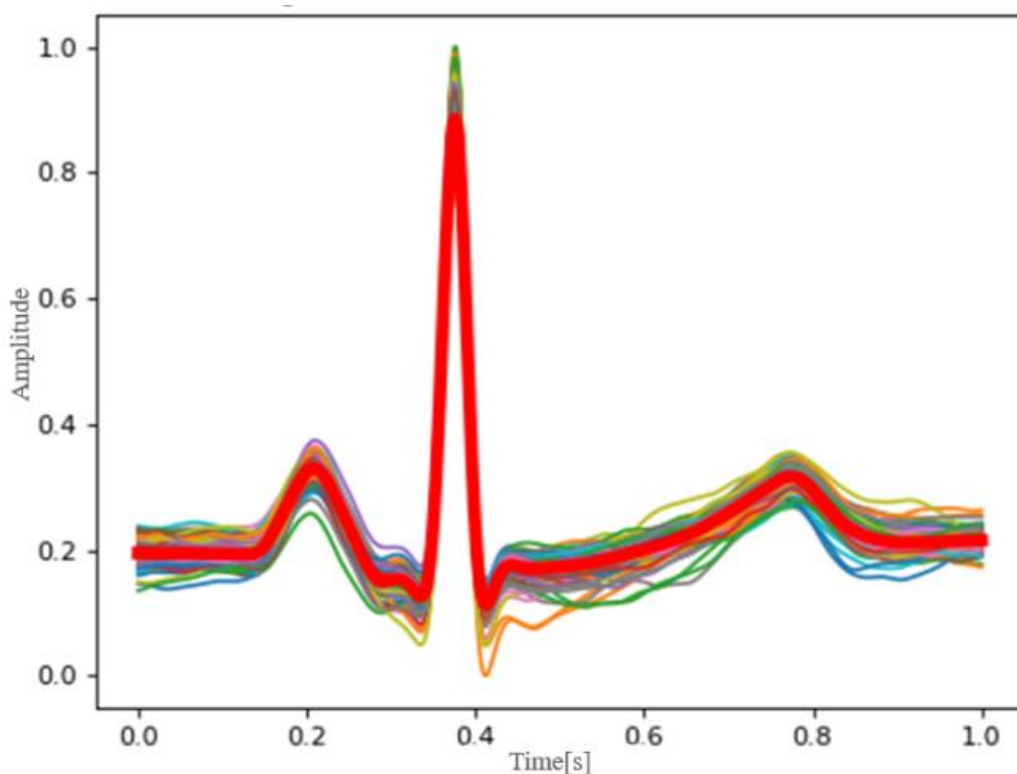


Figure 31. Average waveform for recording 104a, lead II from STAFF III database.

4.3.1 HF Average waveform

The high-frequency average waveform is very similar to the average waveform. Based on the R-peaks, algorithm creates the window and generates a list of waveforms and calculates the average waveform. The difference is that instead of the regularly filtered ECG, HF average waveform is filtered with high-pass-filter of 150 Hz. In figure 32 we can see the HF average waveform.

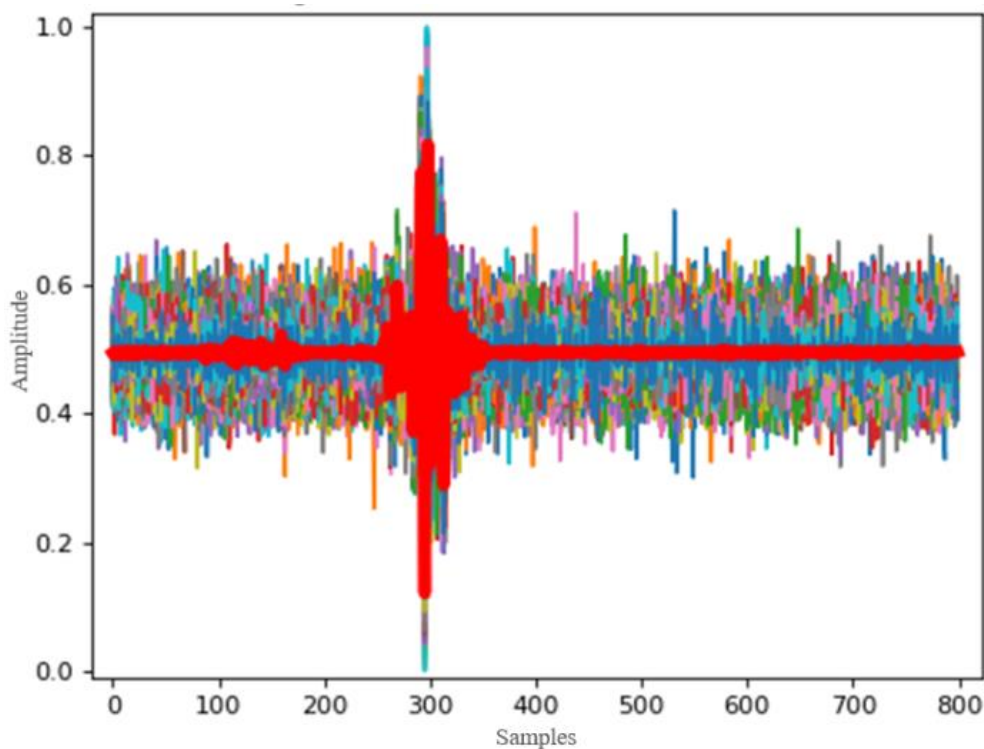


Figure 32. HF average waveform for recording 17a, lead II from STAFF III database.

4.4 P-average waveform

From figures 31 and 32, we can see that the P-waves are also present to some degree. To detect changes in the atrial myocardium, assessment of P-wave is also necessary. The acquirement of the average waveform of the P-wave is similar to the normal average waveform. The window size is smaller, and the reference point is P-peak instead of R-peak. The average waveform of P-wave is shown in figure 33.

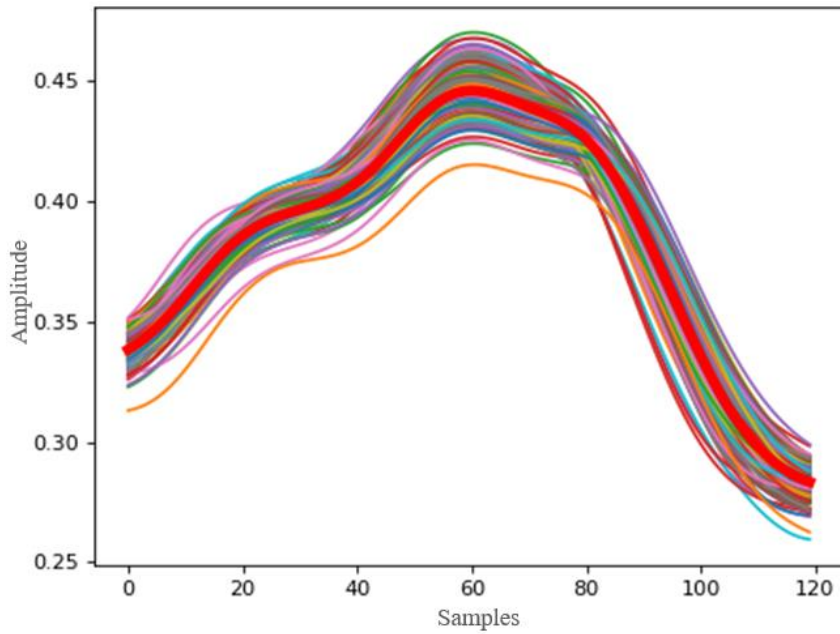


Figure 33. The average waveform of P-waves for recording 17a, lead II from STAFF III database.

4.4.1 HF P-average waveform

The HF average waveform for P-wave is just the high-frequency equivalent of the P-average waveform. For this, the signal is filtered with high-pass-filter of 150 Hz. The average waveform generated can be seen in figure 34.

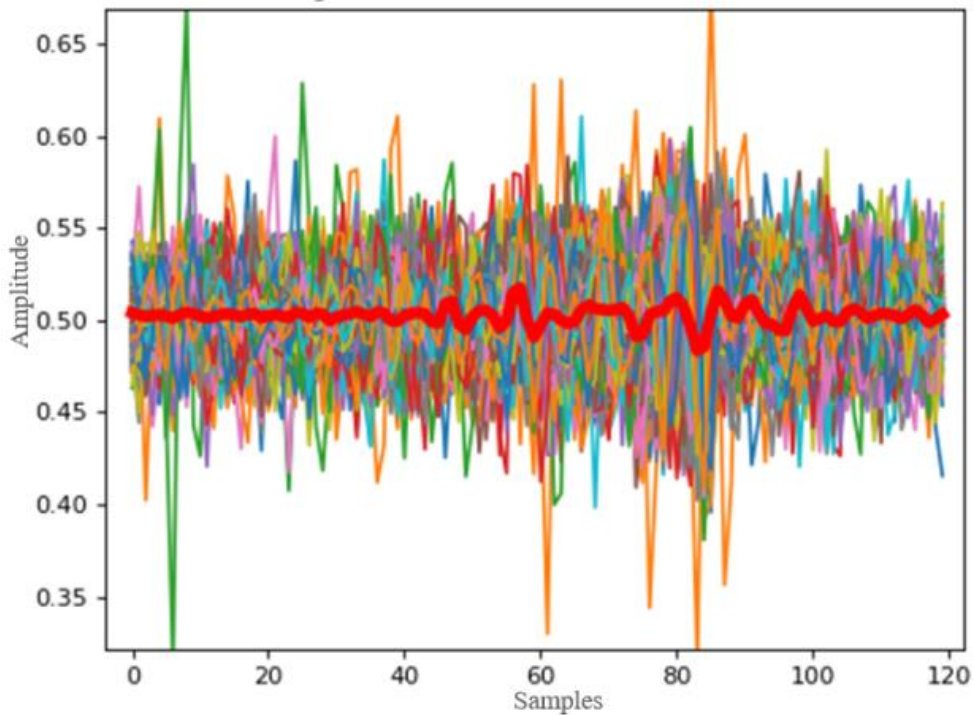


Figure 34. The high-frequency average waveform of P-waves for recording 17a, lead II from STAFF III database.

4.5 Segmentation

It has been proven that assessing the ST-segments changes in ECG is a relevant way to detect AMI [15]. The ECG signals provided in the STAFF III database are 5 minutes long in average, which means that a lot can happen during one ECG recording. In addition to the ST-segments change, the PQ-segment and QRS-complex can change throughout the ECG, especially if an AMI is detected. These are the reasons for segmenting the ECG signals into 30-second-long segments. In figure 35 we can see a 5-minute-long ECG signal segmented into 30-second-long segments.

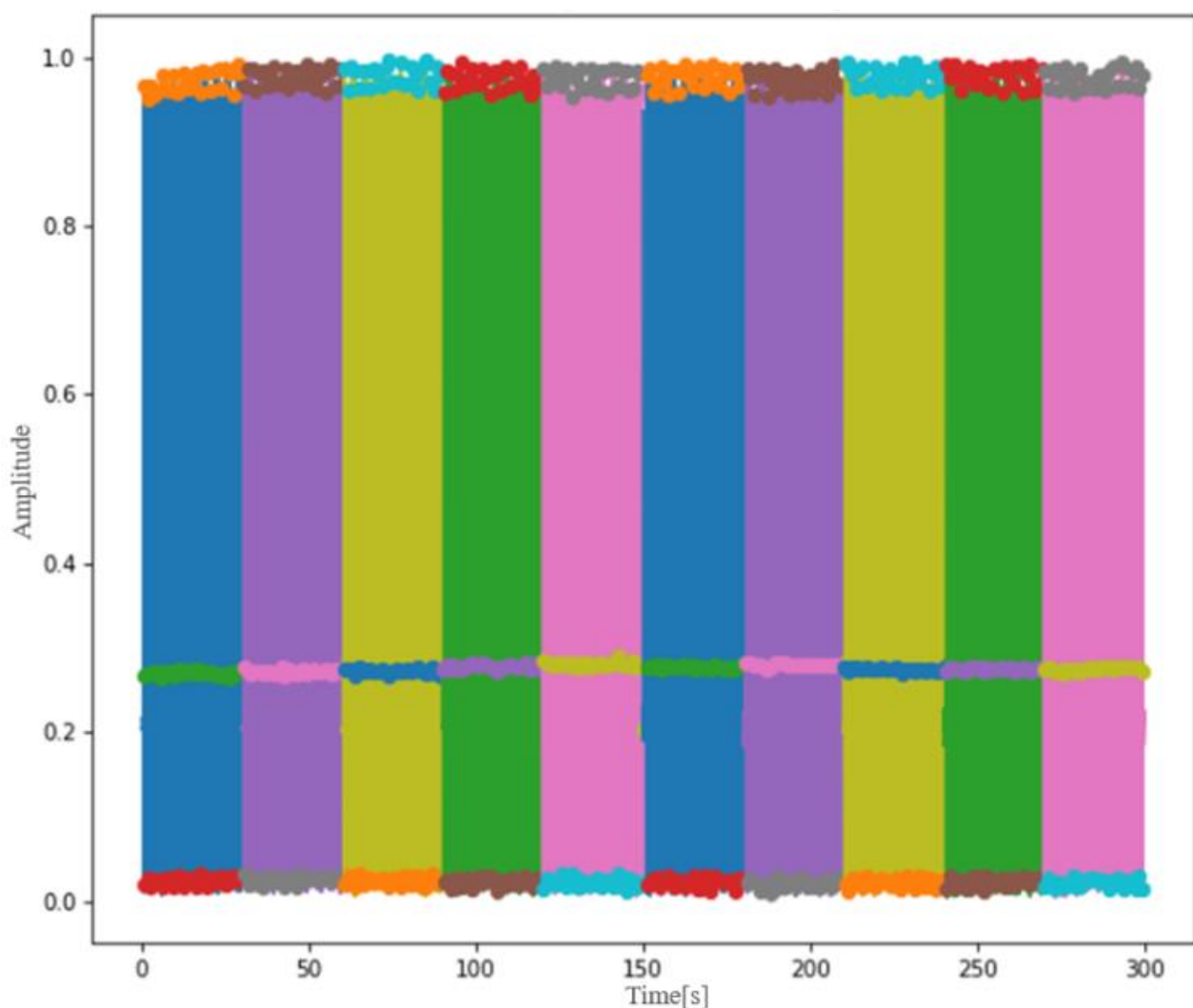


Figure 35. ECG segmented into 30 second epochs. Recording is 9a lead II from STAFF III.

After we have segmented the signal, we take these segments and calculate features within them. The change of different features within the segments is shown in figure 35.

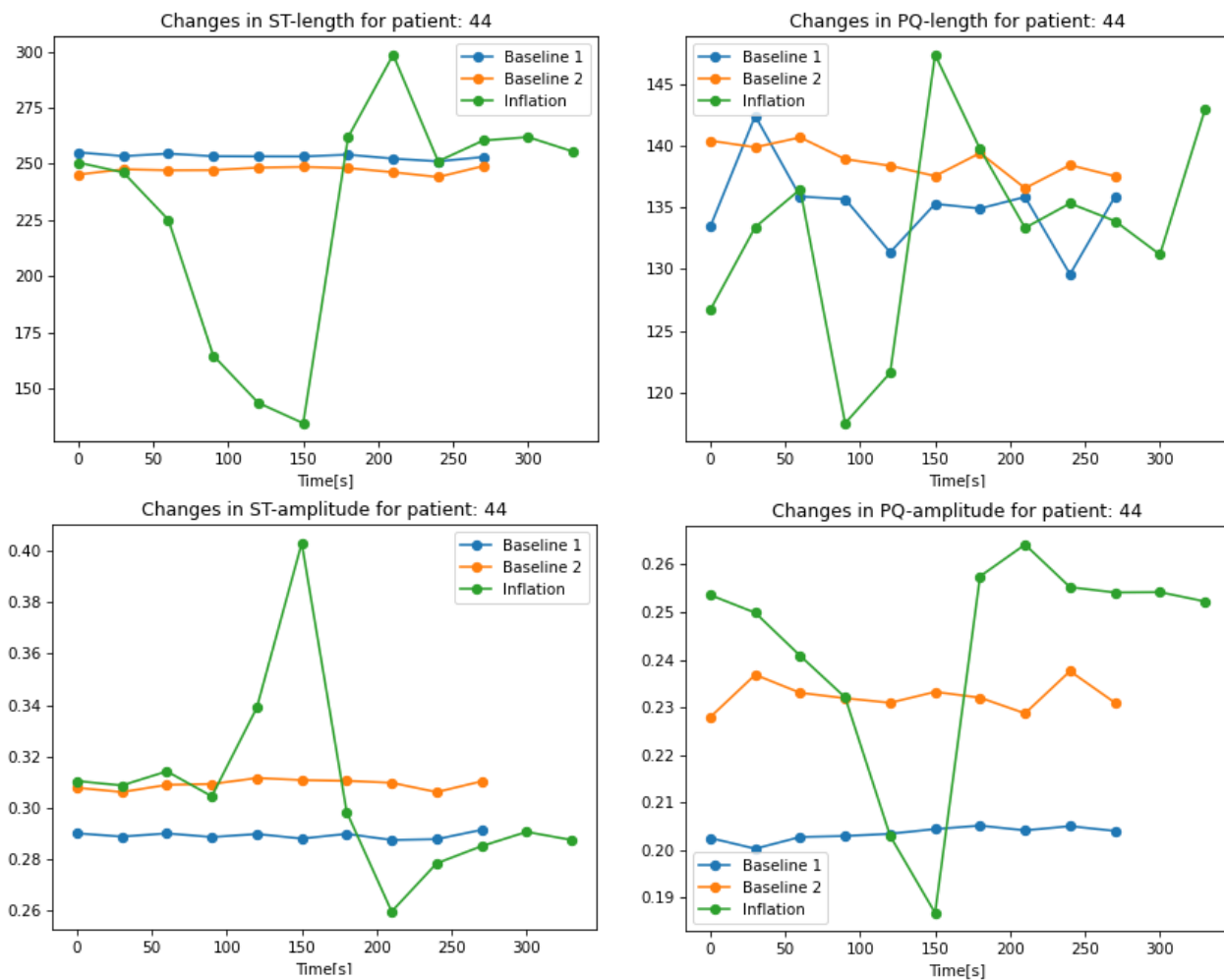


Figure 36. Segmental changes.

In figure 36 we have 4 different features. We have the ST-segments length and amplitude and also the PQ-segments length and amplitude. Every dot in the figure represents a 30-second-long segments average of the specific value. In all of the figures, the baselines consist of 10 dots meaning that they are 5 minutes long, while the inflation in this case is 12 dots and 6 minutes long. The graphs represent the variability of the specific feature over the course of the ECG signal. From figure 36 we can see that the ST-segments of both of the baseline signals stay relatively similar throughout the signal in both amplitude and length. The ST-segments of the inflation ECG however change drastically. We can see that around 55 seconds, the length of the ST-segment drops significantly and returns to normal around 160 second mark. Around 90 second mark, the amplitude of the ST-segment rises significantly and then returns to more stable course after 200 second mark. Similar things happen with the PQ-segment as well. From the STAFF III annotation file, we can see that the patient 44 has his artery occluded from the 0 second mark until 180 second mark. This can somewhat be seen in the figures.

Based on the results of figure 36, we want to calculate the difference and variability of ST- and PQ-segment features within the 30-second segments of the ECG. This is done by adding all of the 30-second segments calculated values into a list, and then calculating the root mean square of the differences between successive segments. Other methods to calculate this variability were used, but this seemed to work most reliability.

5 Feature extraction and selection

5.1 Feature extraction

To evaluate the patients, features from the ECG signals have to be extracted. These features and their values give insightful information of the patient's myocardial health. Feature extraction gives more distinguishable characteristics to the data and makes it easier for the machine learning methods to train.

Multiple different features were extracted from the ECGs of the patients. The extracted features can be divided into five different sections. First section includes the heart rate and heart rate variability features. After the R-peak detection, the HR and HRV features can be extracted. Second feature section focuses on the high-frequency ECG signal. The HF-ECG of the signal is calculated, and then high-frequency features can be extracted. The third section includes the segmentation features. Based on the algorithm shown in chapter 4, the ECG signal is segmented into 30-second-long sections and the features are extracted from the segmented ECG signal. The fourth feature selection includes frequency domain features. Frequency domain was calculated using Welch method and algorithms provided by SciPy's library. The fifth feature section includes average waveform features which are based on the algorithms presented in chapter 4. All of these extracted features are listed below.

1. Heart rate and heart rate variability features

- Heart rate (BPM)
- Root mean square of successive differences (RMSSD)
- Standard deviation of NN intervals (SDNN)
- Spread of RR intervals on the Poincare plot (SD1 and SD2)
- The standard deviation of the successive differences between RR intervals (SDSD)
- The proportion of RR intervals greater than 50ms, out of the total number of RR intervals (pNN50)

- The proportion of RR intervals greater than 20ms, out of the total number of RR intervals. (pNN20)

2. HF-ECG features

- Zero-cross rate of the high-frequency signal
- Root-mean-squared of the high-frequency signal (RMS)
- Absolute energy of the high-frequency signal
- Variance of the high-frequency signal
- Derivative kurtosis of the high-frequency signal

3. Segmentation features

- R-peak amplitude changes in 30-second periods
- ST-segment amplitude changes in 30-second periods
- ST-segments length changes in 30-second periods
- PQ-segments amplitude changes in 30-second periods
- PQ-segments length change in 30-second periods
- Variance of the signal in 30-second periods

4. Frequency domain features

- Median frequency
- Spectral entropy
- Spectral kurtosis
- Dominant frequency

5. Average waveform features

- Slope of average waveform
- Difference of average waveform
- Zero-crossing rate of high-frequency average waveform
- Root-mean-square of high-frequency average waveform
- Kurtosis of high-frequency average waveform
- Variability of high-frequency average waveform
- Slope of P-average waveform
- Absolute energy of high-frequency P-average waveform
- Kurtosis of high-frequency P-average waveform

These features were extracted for 3 different ECG signals for each patient. These signals included the previously mentioned baselines 1 and 2 and also the inflation ECG. After the feature extraction, two different samples for each patient were created. The first one is the healthy sample from the patient, meaning that the features of the baseline 1 were subtracted from features of the baseline 2. The second sample on the other hand was the diseased or the sick sample. In this, the inflation recordings features were subtracted from the features of the baseline 2. After these subtractions, the samples were added to a data frame with the patient's number as a reference, the type of sample as a label and the values of the features as features.

5.2 Feature selection

To make the machine learning process as efficient as possible, the features fed into the machine learning method must be selected carefully. The features have to describe the dataset in the best way possible [68]. The input features can't be irrelevant or redundant. If multiple features have strong correlation between each other, then some of the features might be redundant and can be removed [68].

The feature selection was made manually by evaluating different feature's relevance via correlation heatmaps, boxplots and by trying different combinations for the machine learning. To help the manual evaluation, a feature selection algorithm was run. This was done by Random Forest feature importance algorithm provided by scikit learn. The decisions were made by comparing the importance of the features.

Final features chosen are listed below.

- Root mean square of successive differences (RMSSD)
- Standard deviation of NN intervals (SDNN)
- Zero-cross rate of the high-frequency signal
- Root-mean-squared of the high-frequency signal (HF-RMS)
- Derivative kurtosis of the high-frequency signal
- R-peak amplitude changes in 30 second periods
- ST-segment amplitude changes in 30 second periods
- ST-segments length changes in 30 second periods
- PQ-segments amplitude changes in 30 second periods
- PQ-segments length change in 30 second periods
- Dominant frequency
- Slope of average waveform
- Zero-crossing rate of high-frequency average waveform
- Root-mean-square of high-frequency average waveform
- Kurtosis of high-frequency average waveform
- Slope of high-frequency average waveform

6 SAFE

6.1 SAFE device

SAFE is a single channel ECG measuring necklace developed by the University of Turku. The necklace is based on Suunto's Movesense device and in addition it includes a casing done with 3D printer, two copper leads and a string. The devices two leads can take measurements all over the body. Easiest and the originally intended way to take a measurement is to place the flat side of the device to the patient's chest and then put your finger on the other lead. After both leads detect electric activity, the red indicator LED of the device will start to blink, and the device starts taking the measurement. It will then produce an ECG recording and also accelerometer x-, y- and z-axis recordings. The length and bandwidth of the measurement can be adjusted. It is capable of 128, 256 or 512 Hz sampling frequency [69]. For this study, we used the 512 Hz sampling frequency in order to have the HF-ECG components as well. In figure 37, we can see the SAFE device, its casing and the leads.

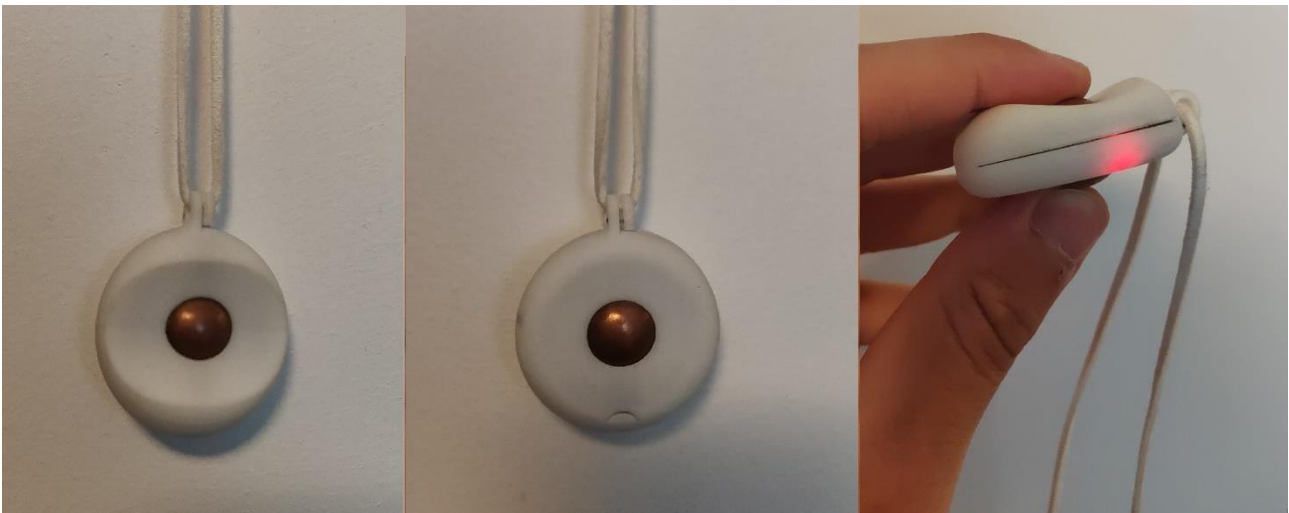


Figure 37. SAFE.

Inside the SAFE necklace there is a device called Movesense medical device (MD) sensor which was developed by Suunto. Movesense is designed to measure ECG and motion signals, which then can be extracted for analysis [69]. It can measure heart rates from 20 BPM to 240 BPM [69]. Movesense MD can also produce clinical grade signals [70] and is classified as a Class IIa medical device [69]. This means that it can't be used as a life sustaining device [69], but can still be valuable. However, it

should not be used as the initial monitoring device in clinical situations and the patient is in risk of severe myocardial injury [69]. The Movesense MD is shown in figure 38.



Figure 38. Movesense MD. Source: [70]

The benefits of Movesense MD is that it is very small, wireless and easily reprogrammable [70]. The diameter is 36.6 mm, 10.6 mm thick and weighs only 9.4 g [70]. It's also very easy to use and the patient can do the measurements himself [69]. After the measurement, the device sends data wirelessly with Bluetooth low energy to a smart phone for example [69][70]. After the transmission, the signal can be stored, processed and analysed in an application [69]. The peak detection and analysing algorithms can be programmed into it [70] and give the patient real time analysis of the condition of his heart. However, in this study the data is extracted from the device, and the analysis is done later. The data comes in .csv files. Depending on the programming, it includes the timestamp, ECG values and 3 different accelerometer values. In this study, we extract only the ECG values and timestamps are added manually.

These kinds of wearable devices could be used to determine the health of the heart easily and with regular measuring to also alarm the patient about potential risks [20]. To be effective, some believe that they should be used daily [21]. Movesense MD is water proof, can sustain reasonable amount of force [70] and has a good battery life which makes it possible for everyday use. However, the device does not automatically measure ECG, it needs to be started voluntarily. With the necklace design, it could become more useful for daily usage. The patient could easily carry it around with him and do a short measurement once a day. This way the analysis could be based on serial ECG as well as initial ECG. The measurement itself is also user friendly, which will be helpful especially with the elder

people [21]. This kind of a necklace also hides the fact that you have a myocardial disease. Some patients may not want to be recognized as cardiac patients [21] and the necklace does not look like a typical ECG device.

6.2 Taking measurements/Data gathering

For this study, I was able to acquire serial-ECG recordings from 10 different people with the SAFE device. This means that for every patient, the ECG was recorded twice. Some patients had measuring interval of 1 hour while some patients had interval of 1 week. This was decided to see if there is a difference regarding the measurement interval. All of the patients were in reasonably good health and did not suffer from any heart diseases.

The measurements were all taken in a resting position, either sitting or lying down. If the first measurement was done while sitting, then also the second measurement was done in the same fashion. The patients were told to relax, while I instructed them on how to use the device. After a quick briefing, the recording could be started. The recordings are 1 minute long, and the patients were instructed to avoid talking or moving unnecessarily during this time. The recordings are taken from the patient's chest. The necklace is placed around the neck and the patients then press down the device to their chest with their index finger of the right hand. The placement on the chest was instructed to be "over the heart". Figure 39 demonstrates how the measurement works with SAFE device.



Figure 39. SAFE measurement.

After the recording is done with the device, it will be connected to a smart phone to which we can download the recording. The recording can be found in the smart phone's data folder as a .csv file. From here, the recording can be transferred to a computer in which we can extract the signal from the .csv file with Python. After the signal is extracted, we can apply our algorithms to that specific signal. In figure 40 we can see an unprocessed ECG signal gathered with the SAFE device.

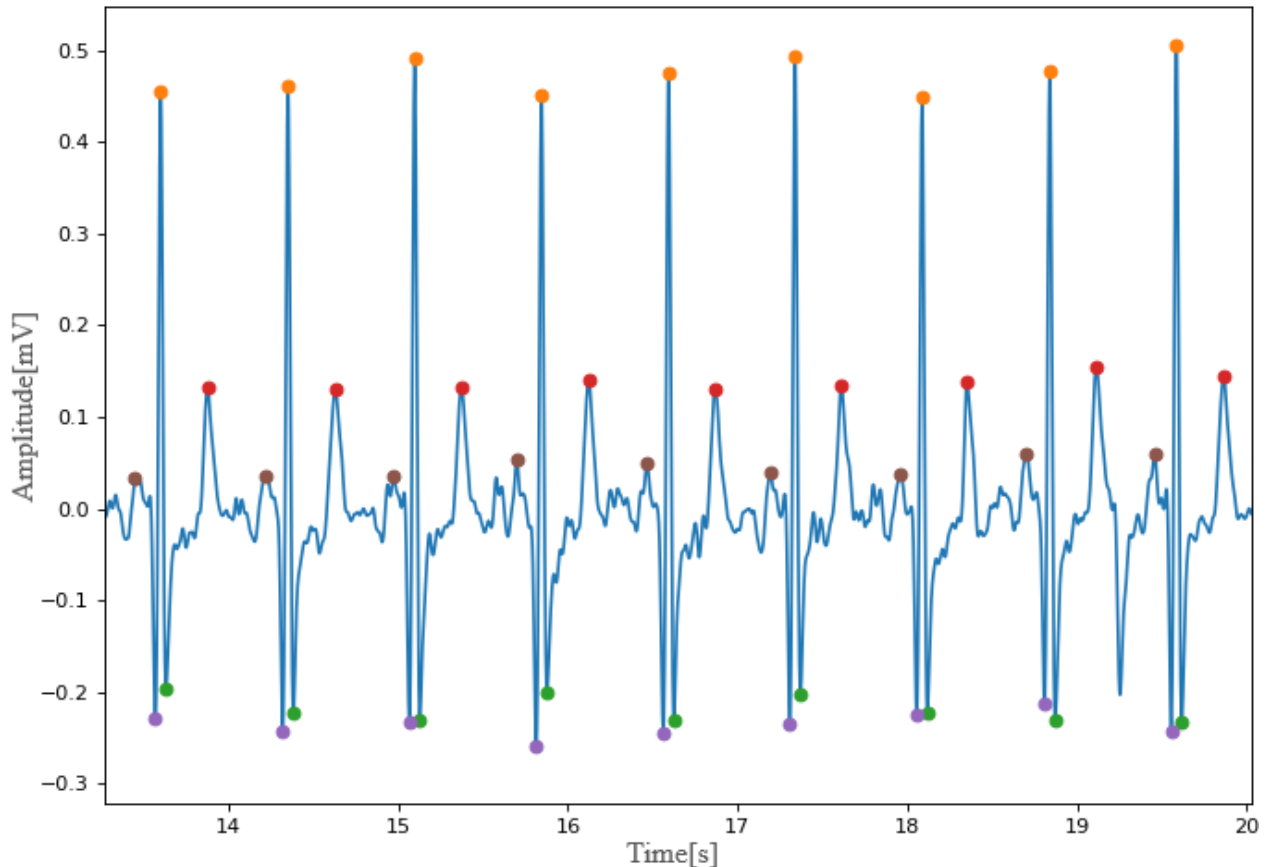


Figure 40. ECG from SAFE device.

From figure 40 we can see that the amplitude created by the device is much different than the ECGs in STAFF III database. Because of this, all of the signals were normalized to limit possible differences due to equipment. The signal in figure 40 is quite clear and including the obvious QRS-complex, we can see the T-waves and even the P-waves quite clearly. For some of the recordings this was not the case however, and only the QRS-complex was easily recognizable, while the T-wave could be spotted but not so clearly and the P-wave was tenuous. A quality check was done for the signals and if it contained any artefacts, the recording was repeated or removed from the database.

7 Results

7.1 Results of STAFF database

From the STAFF dataset, I was able to use 94 different patients. While using 3 different recordings from the patients, I was able to gather 94 healthy cases (baseline2-baseline1) and 94 sick cases (baseline2-inflation). This means that the dataset includes 188 instances. The dataset was split randomly into training set, 75% of the dataset, and a test set, 25% of the dataset. After this the machine learning methods explained in chapter 2.4 were trained with the training set and then tested with the testing set. The results based on these, are shown in the graphs below.

First, these results are presented with confusion matrixes. Confusion matrix is a visual tool that helps to demonstrate the performance of supervised classification machine learning algorithms. In binary classification problem such as ours, it shows the true and false positives and the true and false negatives. With these values, we can calculate the accuracy and other evaluation metrics such as precision, recall and F1 score for the results.

	Predicted Healthy	Predicted inflation
Healthy	22	0
Inflation	6	19

Table 1. K-Nearest Neighbor confusion matrix for STAFF III dataset.

	Predicted Healthy	Predicted inflation
Healthy	21	1
Inflation	3	22

Table 2. Support Vector Classification confusion matrix for STAFF III dataset.

	Predicted Healthy	Predicted inflation
Healthy	21	1
Inflation	3	22

Table 3. Decision tree confusion matrix for STAFF III dataset.

	Predicted Healthy	Predicted inflation
Healthy	20	2
Inflation	1	24

Table 4. Random Forest confusion matrix for STAFF III dataset.

	Predicted Healthy	Predicted inflation
Healthy	21	1
Inflation	1	24

Table 5. Extra Trees confusion matrix for STAFF III dataset.

	Accuracy	Precision	Recall	F1 Score	LOOCV
KNN	87%	89%	88%	87%	91.5%
SVC	91%	92%	92%	91%	93.1%
Decision Tree	94%	94%	93%	94%	93.6%
Random Forest	94%	94%	93%	94%	96.8%
Extra Trees	96%	96%	96%	96%	97.9%

Table 6. Statistics for the different machine learning methods.

Results of the confusion matrixes are similar for all of the machine learning methods. All of them seem to be capable of classifying healthy and inflated ECG signals from each other. However, when looking at the statistics from table 6, we can see that as expected, the most computationally heavy algorithms, Random Forest and Extra Trees, got the best results. However, Decision Tree was not far behind from these two. Extra Trees classifier exceeds the other methods in every aspect based on the statistics. The machine learning methods with lower computational power, KNN and SVC, produced the poorest results. Especially the results of KNN were disappointing.

In table 6, LOOCV represents the accuracy calculated with leave-one-out cross-validation explained in chapter 2.4. Since this dataset was rather small, the LOOCV should produce the most accurate result possible for determining the true accuracy of different machine learning models. With this method, the results correlate strongly with the other evaluation metric values. The computationally heavy methods, Random Forest and Extra Trees, produce the best results.

The number of trees used in the Random Forest and Extra Trees classifiers was 500, meaning that based on the results of 500 Decision Trees, a majority vote was taken, and the classification was based on that. This amount was decided based on the results, while decreasing the number of trees, the accuracy did not significantly decline, but to get the best possible results, 500 trees were chosen. Everything over this number of trees was seen computationally heavy and it took too much time to train the machine learning model compared to the gains in accuracy. For the KNN classifier, the number of the neighbors (k) was 5. This was decided by running an algorithm which tested all k -values between 2-15. The different k -values were run multiple different times in different training and testing set folds, after which the mean accuracy of the results was calculated for each value of k . With this algorithm, k -value of 5 was chosen since it produced the highest accuracy. It still was not able to keep up with the other machine learning methods when looking at the evaluation metrics. The second lowest method was the support vector classifier, which was using a linear kernel. All of the kernel options were tested, but the linear option produced the best results and was chosen.

7.2 Results of SAFE vs STAFF

To be able to answer the research question 2, a dataset gathered with the SAFE device was used as a test set for the machine learning methods. This test set included 10 subjects. The training for these methods was done with the previously mentioned STAFF database, which included 188 subjects. To be able to produce the most accurate results possible, signals from both databases were processed to

be as similar as possible. Before extracting features, all of the signals were normalized, meaning that their amplitudes were fixed between 0 and 1. SAFE signals were also resampled. Since STAFF III database signals had sampling frequency of 1000 Hz, the SAFE device produced a signal with 512 Hz sampling rate. The sampling frequency of STAFF III database was resampled to 512 Hz before the features were extracted.

	Predicted Healthy	Predicted inflation
Healthy	10	0
Inflation	0	0

Table 7. K-Nearest Neighbor confusion matrix when using STAFF as training set and SAFE as test set.

	Predicted Healthy	Predicted inflation
Healthy	9	1
Inflation	0	0

Table 8. Support Vector Classification confusion matrix when using STAFF as training set and SAFE as test set.

	Predicted Healthy	Predicted inflation
Healthy	8	2
Inflation	0	0

Table 9. Decision tree confusion matrix when using STAFF as training set and SAFE as test set.

	Predicted Healthy	Predicted inflation
Healthy	9	1
Inflation	0	0

Table 10. Random Forest confusion matrix when using STAFF as training set and SAFE as test set.

	Predicted Healthy	Predicted inflation
Healthy	9	1
Inflation	0	0

Table 11. Extra Trees confusion matrix when using STAFF as training set and SAFE as test set.

	Accuracy	Precision	Recall	F1 Score
KNN	100%	100%	100%	100%
SVC	90%	100%	90%	94%
Decision Tree	80%	100%	80%	88%
Random Forest	90%	100%	90%	94%
Extra Trees	90%	100%	90%	94%

Table 12. Statistics for the different machine learning methods when using SAFE as test set.

The confusion matrixes show that most of the SAFE measurements get predicted as healthy, as they should be. Differing from the STAFF database results, this time KNN gives us the best results. However, the machine learning models that performed well in the last database are not lagging behind that far. Only one subject is predicted wrong while the others are predicted correctly. Decision Tree gets two subjects wrong, but SVC, Random Forest and Extra Trees get only one subject wrong, which might indicate that it is the same subject in each case. Cross-validation is not used for this database, since it is not a viable option, because the training and test datasets are split in advance.

7.3 Data analysis

Looking and analysing the machine learning results is not the only way to analyse the data. The data can be visualised in different ways and analysed based on this visualization. While visualising the data, we can find the reasons behind the results and see how the data behaves. Correlation, difference, and variation within different data can be seen with the right tools. In the next chapters, some of these tools are presented and the data sets are analysed more deeply.

7.3.1 Principal component analysis

Principal component analysis (PCA) is a dimensional reduction method for data analysis [71]. It takes the features of the data and presents it in 2-dimensional space. This way, the data can be easily presented and analysed in 2D graphs. However even though PCA can be a useful tool, it has its shortcomings. PCA can have trouble with high dimensional data [71], meaning that the 2-dimensional graph presented might not be completely correct. However, it does give a good idea how the data behaves and is a good way to analyse the data, while keeping in mind the shortcomings of the method. In figure 41, we can see the PCA analysis of the combined STAFF III and SAFE database.

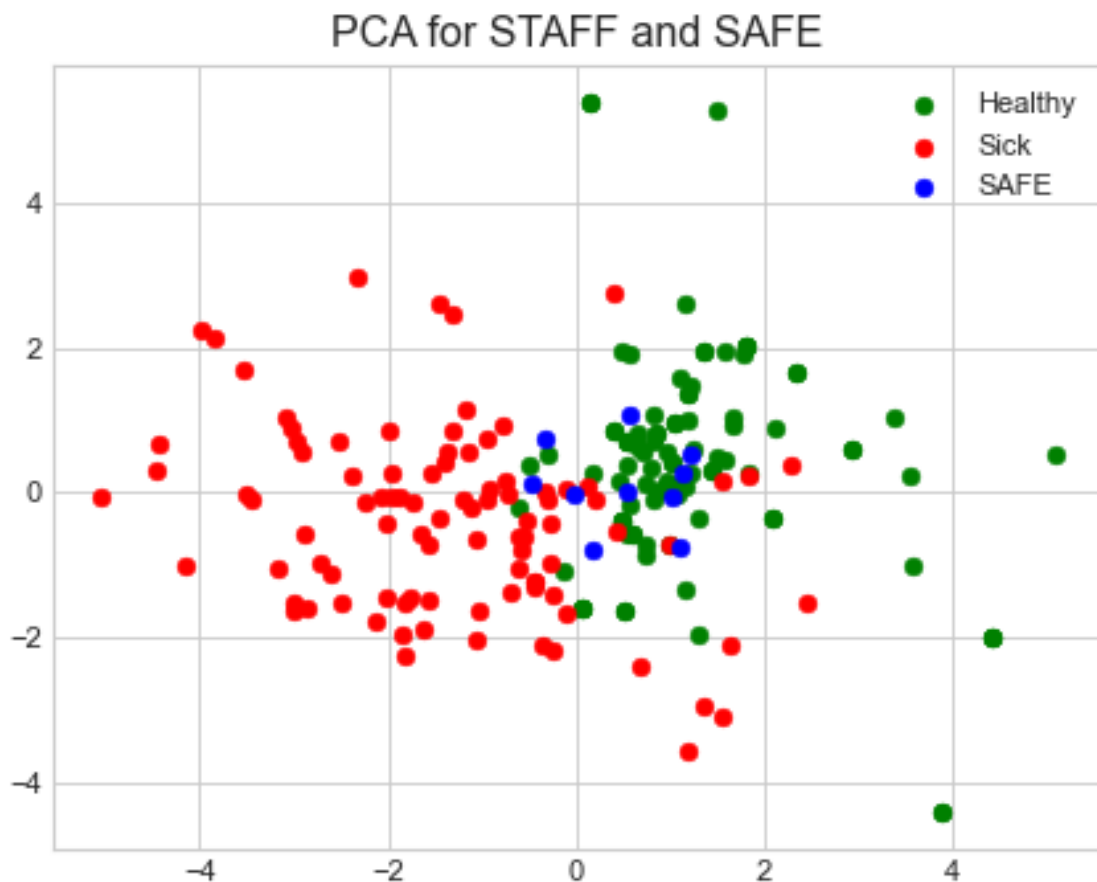


Figure 41. PCA analysis of STAFF and SAFE databases.

From the PCA we can see that the healthy and sick subjects can be distinguished from each other quite easily. The two types of subjects are clearly divided into two different clusters. There are however few instances that overlap a little bit within the clusters, but this is expected. We can also see that the healthy cluster is more compact and has fewer outliers than the inflation cluster. The variation within the inflation cluster is much higher. This indicates that the inflation ECGs are more volatile than the healthy ECGs.

When looking at the SAFE subjects in the PCA figure, we can see that they are mostly located within the healthy cluster. A few subjects are closer to the inflation cluster. However, even in these cases the subjects are close to the healthy cluster. Even though the number of the SAFE subjects is low, we can already see their cluster forming on top of the healthy cluster.

7.3.2 Box plots

Box plot (schematic plot, box-and-whiskers-plot) is one of the simplest tools when analysing the data [72]. However, they are useful in multiple different ways. Box plots show the variation within the specific type of data and the difference between different types of data. It is used to visually identify patterns and attributes within the data [72]. The line in the middle of the box plot represents the median of the data. The coloured box contains 50% of the data, 25% on each side of the median. The so-called whiskers around the box contain 25% of the data in both sides of the box. The dots outside the whiskers are outliers within the data, meaning that they differentiate so much from the rest of the data they are considered as exceptions or miscalculations. Figure 42 shows the box plot of ST-segments amplitude change.

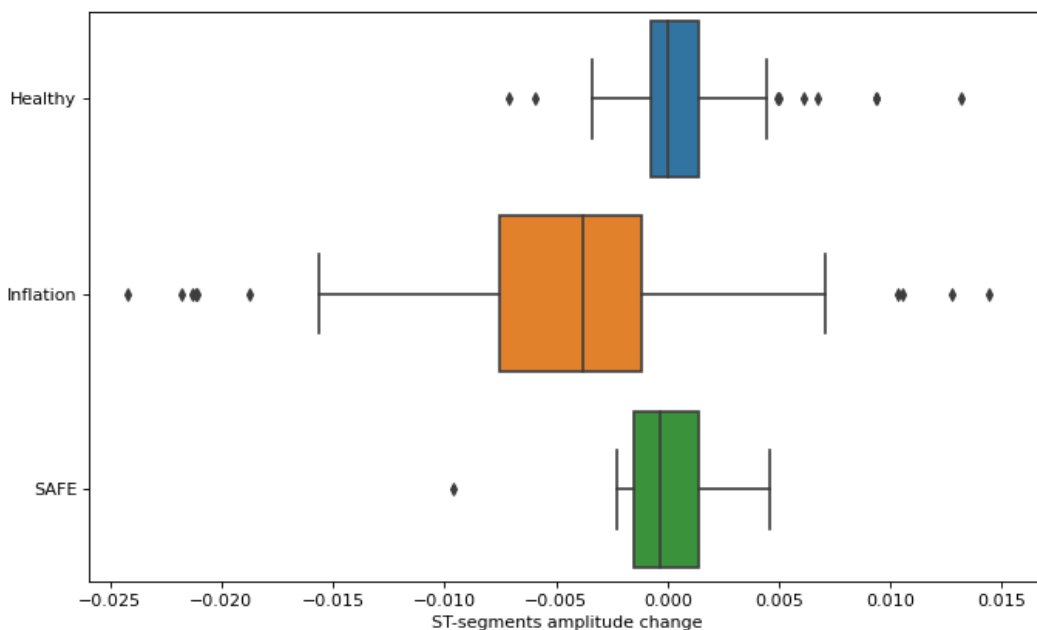


Figure 42. Box plot of ST-segments amplitude change.

From figure 42 we can see that the different sort of data can be distinguished quite clearly from each other. Healthy and inflated data seem to be behaving differently. Healthy subjects seem to be very stable with the amount of change within the ST-segments amplitude, while the inflation subjects seem to have much more change with the amplitude. One thing to note is that the healthy box plot is quite

compact while the inflation box plot is very wide and has a lot of variation. The SAFE box plot seems to be working similarly to the healthy box plot with this particular feature. The variation within both is low. In SAFE box plot, there is one outlier which might indicate a miscalculation with the algorithm or an artefact within one of the signals.

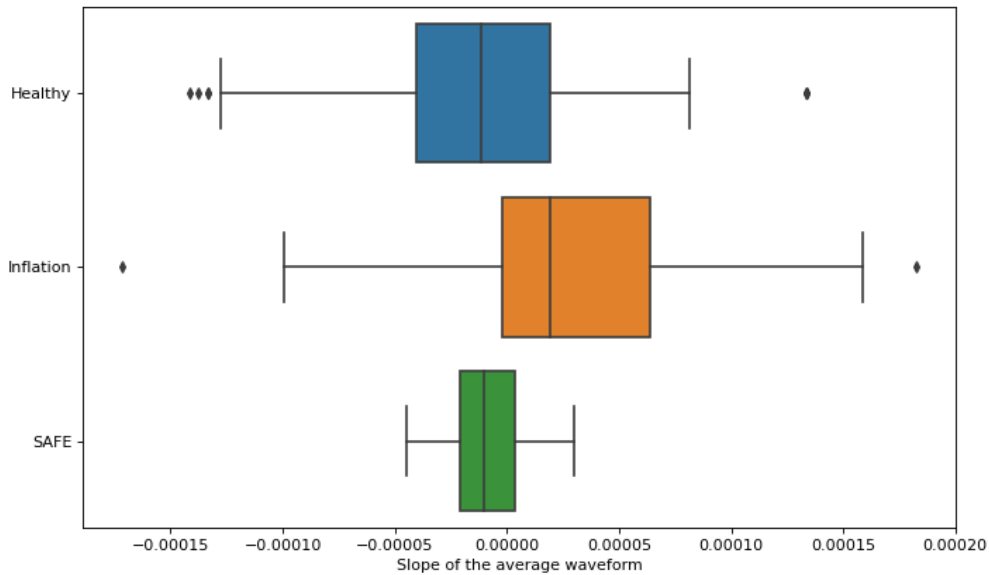


Figure 43. Box plot of the slope of the average waveform.

Figure 43 represents another box plot of the database. From it, we can see that the SAFE and healthy box plots are within the same range, while inflation box has higher values. The variation and overlapping with this particular feature are higher than with ST-segments changes, but the orientation of healthy and inflated features can be seen quite easily.

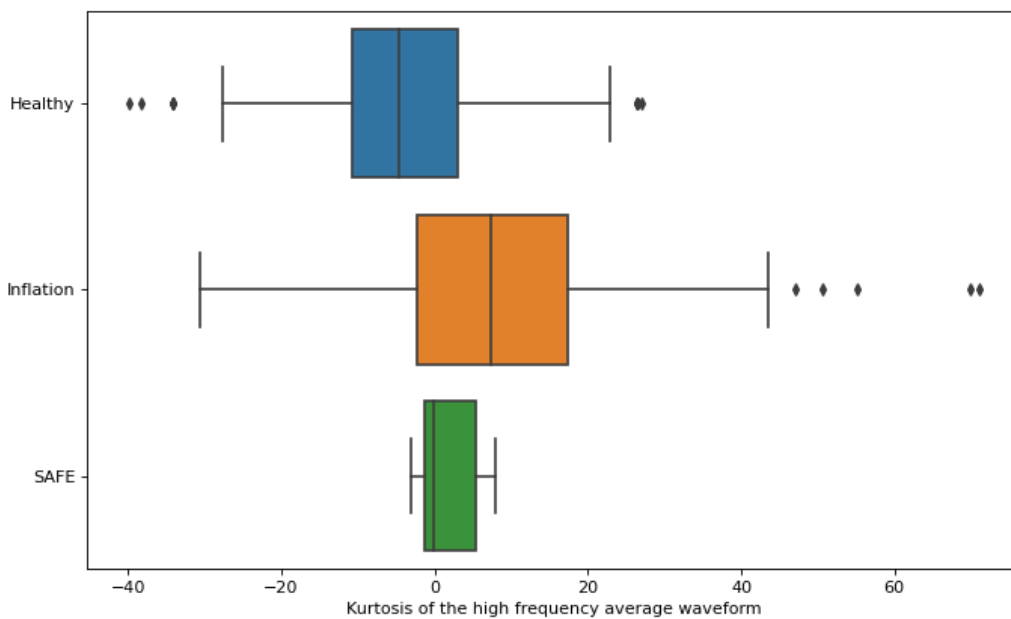


Figure 44. Box plot of the kurtosis of the HF average waveform.

Figure 44 represents a third box plot of the database. This feature works differently, while healthy and inflated subjects are differentiated quite clearly, the SAFE patients overlap between both of them. Some of the features include this sort of overlapping for the SAFE subjects. These box plots represent only three of the features gathered from the signals but demonstrate the data well. Most of the box plots visualised with different features work in similar way. One possible explanation for this could be that the HF contents of the SAFE device might not similar enough to the STAFF III database.

8 Conclusions

In this thesis, we tried to recognize acute myocardial infarctions with serial electrocardiography. For this, we analysed an already existing database and also created our own database with a handheld device. These handheld devices could be a plausible solution when monitoring patients' health [21]. With serial ECG, the measurement could be done once per week and a 30-second-long signal could be sufficient enough to give an estimate on the patient's health, when comparing to older measurements from the same patient.

The subject of high frequency serial electrocardiography is not that well studied. Only a few papers on the subject can be found [18][19][17]. The results of these studies seem to be in line with our results, even though the methods and purposes are a little different. However, these papers conclude that if there is no AMI present, there does not seem to be changes in the HF content of the ECG. While suffering from AMI, the HF-ECG features seem to be affected. This reflects the results of our study. There is still lot to learn about the changes in the HF-ECG, but for now it seems to be an effective way to detect AMI. These new methods could become useful, since the COVID-19 pandemic and its effects on the cardiovascular health [73]. It is shown that the patients infected with COVID-19 are in greater risk of suffering from multiple different cardiovascular diseases [73]. These diseases include myocardial infarction. This new method could become greatly vital, when trying to detect AMI in these types of patients. The possibility to follow the myocardial health of these patients at home would also be highly beneficial. The wearable device used in this thesis could be used for this.

For this thesis, we had two research questions. To answer research question 1, we used STAFF III database to train and test machine learning models in order to classify sick and healthy subjects based on serial electrocardiography. The results we had were good. We were able to identify acute myocardial infarction produced by the balloon inflation with 96% accuracy. The data visualization provides evidence that with the features we extracted from the ECG signals, we were able to clarify a difference between healthy and inflated serial ECG. Even though the results for the STAFF III database were good, we need to keep in mind that we were able to use only 94 subjects, providing a dataset of the size of 188 instances. This is quite small in the perspective of machine learning. In order to get more reliable results, we need to gather a larger dataset including more subjects. However, the results we had from the STAFF III database are promising and are supported by data analysis.

For the research question 2, we gathered data with the SAFE device developed by the University of Turku. I gathered serial-ECG data from 10 different persons and created a dataset with these signals. The machine learning models were trained with the STAFF III database and the dataset I created was used as the training set. The average accuracy of these machine learning models for SAFE data was 90%. Of the 10 patients, 9 were predicted as healthy patients, answering the research question 2. One of the patients was predicted as inflated by many of the machine learning models. When analysing the patients one by one, we can find the patient who is predicted as unhealthy. After seeing the ECG of this patient, we can see the reasons behind the incorrect prediction. The ECG is distorted and has high heart rate variability.

The interval between measurements did not seem to make a difference for the patients. As told in chapter 5.2, some of the patients had 1 hour between the measurements while some of the patients had 1 week or even 1 month between the measurements. This did not affect the results, as for a few of the patients we gathered more than 2 recordings with different measurement intervals, but the results were the same for every interval. The person who got predicted as unhealthy had 1 hour time interval. This patients' ECG was also re-measured, but the results did not change. Even with the new measurement, the patient was predicted as unhealthy.

While analysing the results for the SAFE device, we also have to take into consideration that the dataset gathered by me does not have any acute myocardial infarction patient. All of the subjects who participated in the study were healthy and the measurements were not done within a hospital environment. When we do not have any unhealthy patients for the study, we can't really declare that the SAFE device is able to detect acute myocardial infarction. For that, we would need patients who suffer from this. This could be one thing that could be done in the future. A possible clinical trial which includes inflation or AMI patients with the device would finalize this study and give a definitive answer to this question. This could turn out to be more difficult said than done, since recording ECG while AMI is hard. One other thing to note is also that the dataset size is relatively small. While 90% accuracy is decent, with 10 patients the result might not be the most relevant. With a bigger test set size, we would be able to create a more relevant and accurate prediction of the accuracy of the machine learning models. This is also another thing that could be done in the future. Some other disease recognition such as atrial fibrillation could be done with this device as well in the future.

References

- [1] K. Thygesen, J. S. Alpert, and H. D. White, “Universal Definition of Myocardial Infarction,” *J. Am. Coll. Cardiol.*, vol. 50, no. 22, pp. 2173–2195, 2007, doi: 10.1016/j.jacc.2007.09.011.
- [2] A. Dhawan, B. Wenzel, S. George, I. Gussak, B. Bojovic, and D. Panescu, “Detection of Acute Myocardial Infarction from serial ECG using multilayer support vector machine,” *Proc. Annu. Int. Conf. IEEE Eng. Med. Biol. Soc. EMBS*, pp. 2704–2707, 2012, doi: 10.1109/EMBC.2012.6346522.
- [3] E. Braunwald, “Cardiovascular Medicine at the Turn of the Millennium: Triumphs, Concerns, and Opportunities,” *New England Journal of Medicine*, vol. 337, no. 19, pp. 1360–1369, 1997, doi: 10.1056/nejm199711063371906.
- [4] G. R. Shodieva, A. A. Ruziyeva, B. U. Nizamov, and A. M. Sharipov, “Acute myocardial infarction,” *Int. J. Curr. Res. Rev.*, vol. 12, no. 14, pp. 91–95, 2020, doi: 10.31782/IJCRR.2020.121419.
- [5] D. M. Mirvis and A. L. Goldberger, “Braunwald’s Heart Disease: A Textbook of Cardiovascular Medicine - Electrocardiography,” *Braunwald’s Hear. Dis.*, vol. 9th Editio, pp. 126–167, 2012.
- [6] J. Lehmacher *et al.*, “Predictive Value of Serial ECGs in Patients with Suspected Myocardial Infarction,” *J. Clin. Med.*, vol. 9, no. 7, p. 2303, 2020, doi: 10.3390/jcm9072303.
- [7] A. Sbrollini *et al.*, “Serial electrocardiography to detect newly emerging or aggravating cardiac pathology: A deep-learning approach,” *Biomed. Eng. Online*, vol. 18, no. 15, pp. 1–17, 2019, doi: 10.1186/s12938-019-0630-9.
- [8] P. Jurak *et al.*, “Ultra-high-frequency ECG measurement,” *Comput. Cardiol. (2010).*, vol. 40, pp. 783–786, 2013.
- [9] B. J. A. Schijvenaars, G. van Herpen, and J. A. Kors, “Intraindividual variability in electrocardiograms,” *J. Electrocardiol.*, vol. 41, no. 3, pp. 190–196, 2008, doi: 10.1016/j.jelectrocard.2008.01.012.

- [10] A. Sbröllini *et al.*, “Serial ECG Analysis: Absolute Rather Than Signed Changes in the Spatial QRS-T Angle Should Be Used to Detect Emerging Cardiac Pathology,” *Comput. Cardiol. (2010)*., vol. 2018-Septe, no. January, 2018, doi: 10.22489/CinC.2018.099.
- [11] J. Velez, W. J. Brady, A. D. Perron, and L. Garvey, “Serial electrocardiography,” *Am. J. Emerg. Med.*, vol. 20, no. 1, pp. 43–49, 2002, doi: 10.1053/ajem.2002.28335.
- [12] F. M. Fesmire, R. F. Percy, J. B. Bardoner, D. R. Wharton, and F. B. Calhoun, “Serial ECGs were more sensitive than an initial ECG for diagnosing chest pain,” *Evid. Based. Med.*, vol. 3, no. 4, p. 123, 1998, doi: 10.1136/ebm.1998.3.123.
- [13] M. C. De Jongh, A. C. Maan, E. T. Van Der Velde, and C. A. Swenne, “Serial ECG analysis after myocardial infarction: When heart failure develops, the ECG becomes increasingly discordant,” *Comput. Cardiol. (2010)*., vol. 43, pp. 457–460, 2016, doi: 10.22489/cinc.2016.131-408.
- [14] J. Pettersson *et al.*, “Changes in high-frequency QRS components are more sensitive than ST-segment deviation for detecting acute coronary artery occlusion,” *Journal of the American College of Cardiology*, vol. 36, no. 6. pp. 1827–1834, 2000, doi: 10.1016/S0735-1097(00)00936-0.
- [15] P. Laguna and L. Sörnmo, “The STAFF III ECG database and its significance for methodological development and evaluation,” *J. Electrocardiol.*, vol. 47, no. 4, pp. 408–417, 2014, doi: 10.1016/j.jelectrocard.2014.04.018.
- [16] E. Trägårdh, T. T. Schlegel, M. Carlsson, J. Pettersson, K. Nilsson, and O. Pahlm, “High-frequency electrocardiogram analysis in the ability to predict reversible perfusion defects during adenosine myocardial perfusion imaging,” *J. Electrocardiol.*, vol. 40, no. 6, pp. 510–514, 2007, doi: 10.1016/j.jelectrocard.2007.03.242.
- [17] G. Amit, O. Galante, L. R. Davrath, O. Luria, S. Abboud, and D. Zahger, “High-frequency QRS analysis in patients with acute myocardial infarction: A preliminary study,” *Ann. Noninvasive Electrocardiol.*, vol. 18, no. 2, pp. 149–156, 2013, doi: 10.1111/anec.12023.
- [18] N. J. Batdorf, A. H. Feiveson, and T. T. Schlegel, “Month-to-month and year-to-year reproducibility of high frequency QRS ECG signals.,” *undefined*, vol. 37, no. 4, pp. 289–296, Oct. 2004, doi: 10.1016/J.JELECTROCARD.2004.07.005.

- [19] E. Trägårdh *et al.*, “Serial changes in the high-frequency ECG during the first year following acute myocardial infarction,” *Clin. Physiol. Funct. Imaging*, vol. 26, no. 5, pp. 296–300, 2006, doi: 10.1111/j.1475-097X.2006.00691.x.
- [20] S. Nagai, D. Anzai, and J. Wang, “Motion artefact removals for wearable ECG using stationary wavelet transform,” doi: 10.1049/htl.2016.0100.
- [21] O. E. Santala *et al.*, “Necklace-embedded electrocardiogram for the detection and diagnosis of atrial fibrillation,” *Clin. Cardiol.*, vol. 44, no. 5, pp. 620–626, 2021, doi: 10.1002/clc.23580.
- [22] D. E. Becker, “Fundamentals of electrocardiography interpretation,” *Anesth. Prog.*, vol. 53, no. 2, pp. 53–64, 2006, doi: 10.2344/0003-3006(2006)53[53:FOEI]2.0.CO;2.
- [23] Y. C. Yeh and W. J. Wang, “QRS complexes detection for ECG signal: The Difference Operation Method,” *Comput. Methods Programs Biomed.*, vol. 91, no. 3, pp. 245–254, 2008, doi: 10.1016/j.cmpb.2008.04.006.
- [24] I. I. Christov, “Real time electrocardiogram QRS detection using combined adaptive threshold,” *Biomed. Eng. Online*, vol. 3, pp. 1–9, 2004, doi: 10.1186/1475-925X-3-28.
- [25] F. Censi *et al.*, “P-wave Variability and Atrial Fibrillation,” *Sci. Rep.*, vol. 6, pp. 1–7, 2016, doi: 10.1038/srep26799.
- [26] M. R. Boyett, H. Honjo, and I. Kodama, “The sinoatrial node, a heterogeneous pacemaker structure,” *Cardiovasc. Res.*, vol. 47, no. 4, pp. 658–687, 2000, doi: 10.1016/S0008-6363(00)00135-8.
- [27] E. Hartmann, “ECG front-end design is simplified with microconverter,” *Analog Dialogue*, pp. 1–5, 2003, [Online]. Available: http://d1.amobbs.com/bbs_upload782111/files_46/ourdev_680028HHNGNM.pdf.
- [28] Andrew G. Webb, *Principles of Biomedical Instrumentation*. 2018.
- [29] F. Buendía-Fuentes *et al.*, “High-Bandpass Filters in Electrocardiography: Source of Error in the Interpretation of the ST Segment,” *ISRN Cardiol.*, vol. 2012, pp. 1–10, 2012, doi: 10.5402/2012/706217.

- [30] K. Yodogawa *et al.*, “Prediction of atrial fibrillation after ischemic stroke using P-wave signal averaged electrocardiography,” *J. Cardiol.*, vol. 61, no. 1, pp. 49–52, 2013, doi: 10.1016/j.jjcc.2012.08.013.
- [31] M. Saleh and J. A. Ambrose, “Understanding myocardial infarction [version 1; referees: 2 approved],” *F1000Research*, vol. 7, no. 0, pp. 1–8, 2018, doi: 10.12688/f1000research.15096.1.
- [32] “STAFF III Database v1.0.0.” <https://physionet.org/content/staffiii/1.0.0/> (accessed Jul. 13, 2021).
- [33] S. H. A. Kazmi *et al.*, “The angelmed guardian® system in the detection of coronary artery occlusion: Current perspectives,” *Med. Devices Evid. Res.*, vol. 13, pp. 1–12, 2020, doi: 10.2147/MDER.S219865.
- [34] Š. Grmec, “Painless acute myocardial infarction and diabetes mellitus,” *Crit. Care*, vol. 2, no. Suppl 1, p. P052, 1998, doi: 10.1186/CC182.
- [35] S. A. K. Nishtar, “Painless myocardial infarction,” vol. 4, no. 4, 2013, doi: 10.1097/00000441-194005000-00004.
- [36] A. Wu *et al.*, “Initial Experience in Monitoring QT Intervals Using a Six-lead Contactless Mobile Electrocardiogram in an Inpatient Setting,” *Nature*, vol. 388, pp. 1–14, 2020.
- [37] B. Krzowski *et al.*, “Kardia Mobile and ISTEEL HR applicability in clinical practice: a comparison of Kardia Mobile, ISTEEL HR, and standard 12-lead electrocardiogram records in 98 consecutive patients of a tertiary cardiovascular care centre,” *Eur. Hear. J. - Digit. Heal.*, 2021, doi: 10.1093/ehjdh/ztab040.
- [38] “(5) How Does HeartBeam’s iCardiologist™ Work? | LinkedIn.” <https://www.linkedin.com/pulse/how-does-heartbeams-icardiologist-work-branislav-vajdic/> (accessed Sep. 08, 2021).
- [39] AliveCor, “KardiaMobile 6L.” <https://shop.de.alivecor.com/products/kardiamobile6l>.
- [40] E. Martegani, D. Porro, B. M. Ranzi, L. Alberghina, and S. Biochimica, “Sampling, Data Transmission, and the Nyquist Rate.”

- [41] HeartBeam, “HeartBeam.” <https://www.heartbeam.com/#HeartBeam>.
- [42] “HeartBeam photo.” <https://www.scripttic.com/project-revealed-heartbeam/>.
- [43] F. Van Heuverswyn *et al.*, “Feasibility and performance of a device for automatic self-detection of symptomatic acute coronary artery occlusion in outpatients with coronary artery disease: a multicentre observational study,” *Lancet Digit. Heal.*, vol. 1, no. 2, pp. e90–e99, 2019, doi: 10.1016/S2589-7500(19)30026-3.
- [44] E. H. M *et al.*, “Diagnostic accuracy of a novel method for detection of acute transmural myocardial ischemia based upon a self-applicable 3-lead configuration,” *J. Electrocardiol.*, vol. 49, no. 2, pp. 192–201, Mar. 2016, doi: 10.1016/J.JELECTROCARD.2015.11.007.
- [45] “RELF project.” <https://relf.eu/relf-device>.
- [46] M. C. Day and C. Young, “This is your heart speaking. Call 911.,” *Ergon. Des.*, vol. 20, no. 2, pp. 4–12, 2012, doi: 10.1177/1064804611435652.
- [47] A. Samol, K. Bischoff, B. Luani, D. Pascut, M. Wiemer, and S. Kaese, “Recording of bipolar multichannel ECGs by a smartwatch: Modern ECG diagnostic 100 years after Einthoven,” *Sensors (Switzerland)*, vol. 19, no. 13, 2019, doi: 10.3390/s19132894.
- [48] C. Indolfi *et al.*, “Multichannel Electrocardiograms Obtained by a Smartwatch for the Diagnosis of ST-Segment Changes,” *JAMA Cardiol.*, vol. 5, no. 10, pp. 1176–1180, 2020, doi: 10.1001/jamacardio.2020.3994.
- [49] K. Stark, T. Czermak, S. Massberg, and M. Orban, “Watch out for ST-elevation myocardial infarction: A case report of ST-elevation in single-lead electrocardiogram tracing of a smartwatch,” *Eur. Hear. J. - Case Reports*, vol. 4, no. 6, pp. 1–4, 2020, doi: 10.1093/ehjcr/ytaa353.
- [50] “Apple Health application.” <https://support.apple.com/en-us/HT208955>.
- [51] S. Shalev-Shwartz and S. Ben-David, *Understanding machine learning: From theory to algorithms*, vol. 9781107057. 2013.
- [52] H. Bhavsar and A. Ganatra, “A Comparative Study of Training Algorithms for Supervised Machine Learning,” *Int. J. Soft Comput. Eng.*, vol. 2, no. 4, pp. 74–81, 2012.

- [53] “scikit-learn: machine learning in Python — scikit-learn 1.0.1 documentation.” <https://scikit-learn.org/stable/> (accessed Dec. 16, 2021).
- [54] C. Crisci, B. Ghattas, and G. Perera, “A review of supervised machine learning algorithms and their applications to ecological data,” *Ecol. Modell.*, vol. 240, no. June 2018, pp. 113–122, 2012, doi: 10.1016/j.ecolmodel.2012.03.001.
- [55] N. Sharma, “Understanding the Mathematics behind Support Vector Machines,” 2020. <https://heartbeat.fritz.ai/understanding-the-mathematics-behind-support-vector-machines-5e20243d64d5>.
- [56] L. Machines, “Chapter 6 Support Vector Machines,” pp. 1–11, 2009.
- [57] P. Aznar, “What is the difference between Extra Trees and Random Forest? | Quantdare,” 2020. <https://quantdare.com/what-is-the-difference-between-extra-trees-and-random-forest/> (accessed Dec. 15, 2021).
- [58] D. Berrar, “Cross-validation,” *Encycl. Bioinforma. Comput. Biol. ABC Bioinforma.*, vol. 1–3, no. January 2018, pp. 542–545, 2018, doi: 10.1016/B978-0-12-809633-8.20349-X.
- [59] J. P. Martínez, O. Pahlm, M. Ringborn, S. Warren, P. Laguna, and L. Sörnmo, “The STAFF III Database: ECGs recorded during acutely induced myocardial ischemia,” *Comput. Cardiol. (2010)*, vol. 44, no. Lcx, pp. 1–4, 2017, doi: 10.22489/CinC.2017.266-133.
- [60] C. Indy *et al.*, “The New England Journal of Medicine CORONARY ANGIOPLASTY WITH OR WITHOUT STENT IMPLANTATION FOR ACUTE MYOCARDIAL INFARCTION A BSTRACT,” 1999.
- [61] “Angioplasty photo.” [Online]. Available: <https://upload.wikimedia.org/wikipedia/commons/6/68/Angioplasty-scheme.svg>.
- [62] “wfdb — wfdb 3.4.0 documentation.” <https://wfdb.readthedocs.io/en/latest/> (accessed Jul. 16, 2021).
- [63] M. H. Sedaaghi, “An efficient ECG background normalization,” *13th Eur. Signal Process. Conf. EUSIPCO 2005*, no. July, pp. 5–8, 2005.
- [64] S. I. Purnama, H. Kusuma, and T. A. Sardjono, “Electrocardiogram Feature Recognition

- Algorithm with Windowing and Adaptive Thresholding,” *J. Phys. Conf. Ser.*, vol. 1201, no. 1, 2019, doi: 10.1088/1742-6596/1201/1/012048.
- [65] J.-S. Park, S.-W. Lee, and U. Park, “R Peak Detection Method Using Wavelet Transform and Modified Shannon Energy Envelope,” 2017, doi: 10.1155/2017/4901017.
- [66] “scipy.signal.find_peaks — SciPy v1.7.0 Manual.”
https://docs.scipy.org/doc/scipy/reference/generated/scipy.signal.find_peaks.html (accessed Jul. 16, 2021).
- [67] G. Turitto, R. Abdula, D. Benson, and N. El-Sherif, “Signal averaged electrocardiogram,” *Electr. Dis. Hear. Genet. Mech. Treat. Prev.*, vol. 27, no. 1, pp. 353–364, 2008, doi: 10.1007/978-1-84628-854-8_24.
- [68] “Data Preparation for Machine Learning: Data Cleaning, Feature Selection, and ... - Jason Brownlee - Google Books.”
https://books.google.fi/books?hl=en&lr=&id=uAPuDwAAQBAJ&oi=fnd&pg=PP1&dq=feature+selection+python&ots=C13GwhdOxW&sig=PjnMDv3H0kmIEGycborZIpP42HY&redir_esc=y#v=onepage&q&f=false (accessed Sep. 24, 2021).
- [69] “MOVESENSE MD User Guide,” 2020, [Online]. Available:
<https://www.movesense.com/wp-content/uploads/2021/02/Movesense-MD-User-Guide-R78-Public.pdf>.
- [70] B. Le and O. Apis, “Movesense MD is a wireless programmable sensor , used an ECG and movement signal,” pp. 12–13, 2020.
- [71] S. Roweis, “EM algorithms for PCA and SPCA,” *Adv. Neural Inf. Process. Syst.*, pp. 626–632, 1998.
- [72] D. F. Williamson, R. A. Parker, and J. S. Kendrick, “The box plot: A simple visual method to interpret data,” *Ann. Intern. Med.*, vol. 110, no. 11, pp. 916–921, 1989, doi: 10.7326/0003-4819-110-11-916.
- [73] Y. Xie, E. Xu, B. Bowe, and Z. Al-Aly, “Long-term cardiovascular outcomes of COVID-19,” *Nat. Med.*, vol. 2019, 2022, doi: 10.1038/s41591-022-01689-3.

Attachments

STAFF III database annotations

The full annotation table can be found at: <https://physionet.org/content/staffiii/1.0.0/>

Patient	Age	Sex	Type of recording and related filenames						
			Baseline room (BR)	Baseline (BC)	cathlab	Balloon inflation (BI)			
#			BR	BC1	BC2	BI1	BI2	BI3	BI4
1	52	f	1a	1b		1c			
2	77	m	2a	2b	2c	2d	2e		
3	77	f	3a	3b		3c			
4	45	f		4a	4b	4c			
5	72	m		5a	5b	5c			
6	75	m		6a	6b	6c			
7	66	m	7a	7b		7c	7c		
8	45	m	8a	8b		8c	8d	8e	
9	46	f	9a	9b		9c			
10	54	f	10a	10b		10c			
11	100	m	11a	11b		11c	11c	11d	
12	67	m	12a	12b		12c			
13	78	m	13a	13b		13c	13d	13e	13f
14	?	m	14a	14b		14c	14d		
15	?	m	15a	15b		15c			
16	47	m	16a	16b		16c			
17	57	m	17a	17b		17c			
18	77	f		18a		18b			
19	60	m	19a	19b		19c			
20	52	f	20a	20b		20c	20d		
21	38	m		21a	21b	21c			
22	65	m	22a	22b	22c	22d			
23	56	f	23a	23b		23c			
24	53	f	24a	24b		24c	24d		
25	74	f	25a	25b		25c			
26	48	m	26a	26b		26c			
27	66	f	27a	27b		27c			
28									
29	55	f	29a	29b		29c	29c		
30	63	f	30a	30b		30c			
31	72	f		31a	31b	31c	31c		
32	51	m	32a	32b		32c	32d		
33	56	m	33a	33b		33c	33d		
34	54	f		34a		34b			
35	67	m	35a	35b		35c	35d		
36	59	m	36a	36b		36c			

37	77	f	37a	37b		37c			
38	60	m	38a			38b			
39	48	m	39a	39b		39c	39c	39c	39d
40	49	m	40a	40b		40c	40d		
41	67	f	41a	41b		41c			
42	53	f	42a	42b		42c	42d		
43	55	m	43a	43b		43c			
44	62	m	44a	44b		44c			
45	67	m		45a		45b	45c		
46	70	f	46a	46b		46c	46d		
47	43	f	47a	47b		47c	47d		
48	48	m	48a	48b		48c			
49	51	f		49a		49b	49c		
50	48	m	50a	50b		50c			
51	67	m	51a	51b		51c			
52	59	m		52a	52b	52c			
53	68	m	53a	53b		53c	53c		
54	51	m	54a	54b		54c	54e		
55	63	m		55a		55b			
56	60	m		56a		56b			
57	73	f	57a	57b		57c			
58	58	m		58a		58b			
59	59	m		59a		59b	59c	59d	
60	58	f		60a		60b			
61	70	m		61a		61b			
62	71	m		62a		62b	62c		
63	65	f		63a		63b			
64	51	f		64a		64b	64b	64c	
65	58	m	65a	65b		65c			
66	53	m	66a	66b		66c			
67									
68	63	f	68a	68b		68c			
69	78	f	69a	69b		69c			
70	70	m		70a		70b			
71	44	m	71a	71b		71c			
72	63	f	72a	72b		72c			
73	63	m	73a	73b		73c	73d	73e	
74	56	f	74a	74b		74c			
75	70	f		75a		75b			
76	85	f	76a	76b		76c	76d		
77	61	m	77a	77b		77c	77c		
78									
79	77	m	79a	79b		79c			
80	59	m	80a	80b		80c			
81	72	m	81a	81b		81c	81d		
82	80	m		82a	82b	82c	82d		
83	52	m	83a	83b		83c			
84	72	m		84a		84b			

85	61	m		85a		85b	85c		
86	46	f		86a		86b	86c		
87	54	m		87a	87b	87c			
88	40	m		88a		88b			
89	57	m	89a	89b		89c	89d		
90	62	m	90a	90b		90c	90d	90e	
91	39	m	91a	91b		91c			
92	56	m	92a	92b		92c			
93	68	f	93a	93b		93c			
94	61	f	94a	94b		94c			
95	69	f	95a	95b		95c			
96	76	m	96a	96b		96c	96d	96e	
97	57	m	97a	97b		97c			
98	53	f	98a	98b		98c			
99	50	m	99a	99b		99c			
100	75	m		100a		100b	100c		
101	63	f		101a		101b			
102	63	m	102a	102b		102c			
103									
104	74	f	104a	104b		104c			
105	32	m		105a		105b			
106	70	m	106a	106b		106c			
107	53	f		107a	107b	107c			
108	49	m	108a	108b		108c			